Navy Experimental Diving Unit (NEDU)
321 Bullfinch Rd.
Panama City, FL 32407-7015

TA 01-07
NEDU TR 04-41
December 2004

A SIMPLE PROBABILISTIC MODEL FOR ESTIMATING THE RISK OF STANDARD AIR DIVES

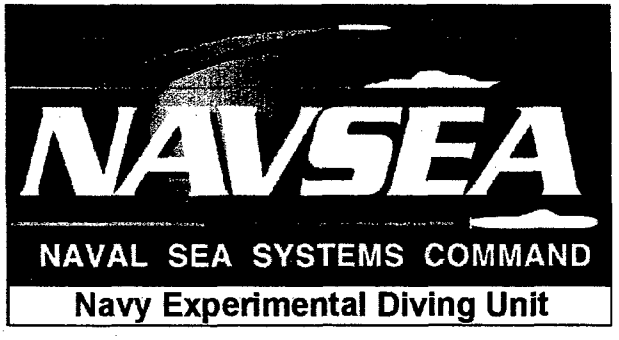

Authors: H. D. Van Liew, Ph.D.
E. T. Flynn, M.D.

REPORT DOCUMENTATION PAGE

1a. REPORT SECURITY CLASSIFICATION Unclassified	1b. RESTRICTIVE MARKINGS
2a. SECURITY CLASSIFICATION AUTHORITY	3. DISTRIBUTION/AVAILABILITY OF REPORT DISTRIBUTION STATEMENT A: Approved for public release; distribution is unlimited.
2b. DECLASSIFICATION/DOWNGRADING AUTHORITY	
4. PERFORMING ORGANIZATION REPORT NUMBER(S) NEDU Technical Report No. 04-41	5. MONITORING ORGANIZATION REPORT NUMBER(S)
6a. NAME OF PERFORMING ORGANIZATION Navy Experimental Diving Unit 6b. OFFICE SYMBOL (If Applicable)	7a. NAME OF MONITORING ORGANIZATION
6c. ADDRESS (City, State, and ZIP Code) 321 Bullfinch Road, Panama City, FL 32407-7015	7b. ADDRESS (City, State, and Zip Code)
8a. NAME OF FUNDING SPONSORING ORGANIZATION Naval Sea Systems Command 8b. OFFICE SYMBOL (If Applicable) 00C	9. PROCUREMENT INSTRUMENT IDENTIFICATION NUMBER
8c. ADDRESS (City, State, and ZIP Code) 1333 Isaac Hull Avenue SE, Washington Navy Yard, DC 20376-1073.	10. SOURCE OF FUNDING NUMBERS Naval Sea Systems Command

PROGRAM ELEMENT NO.	PROJECT NO.	TASK NO.	WORK UNIT ACCESSION NO.
0603713N	S0099	01A	**99-04 & (01-07)**

11. TITLE (Include Security Classification)
(U) **A Simple Probabilistic Model For Estimating The Risk Of Standard Air Dives**

12. PERSONAL AUTHOR(S)
H. D. VAN LIEW, Ph.D.; E. T. FLYNN, M.D.

13a. TYPE OF REPORT	13b. TIME COVERED	14. DATE OF REPORT (Day, Month, Year)	15. PAGE COUNT
Technical Report	FROM 1997 to 2002	December 2004	49

16. SUPPLEMENTARY NOTATION

17. COSATI CODES			18. SUBJECT TERMS (Continue on reverse if necessary and identify by block number)
FIELD	GROUP	SUB-GROUP	Bends, decompression sickness, probabilistic models, standard air dives, undersea medicine

19. ABSTRACT. Statistical fitting of an algorithm to "calibration data" gives parameter values for a "probabilistic decompression model." Some previous probabilistic models prescribe long times at decompression stops for standard air dives. Here we present a simple model, based on premises different from those used previously, to test whether long decompression times are necessary and to enable risk of decompression sickness (DCS) to be estimated in air dives. Using logistic regression, we focus on the total times spent at decompression stops. For calibration data, we use carefully controlled experimental dives recorded in the U.S. Navy Decompression Database in the range of standard air dives, but we exclude saturation and repetitive dives. To evaluate the model, we display its prescriptions for total decompression time along with individual dive-outcome points from the calibration data. Chi-square analyses and graphs of predicted versus observed DCS incidence as functions of depth, bottom time, and time at decompression stops show that our model agrees well with the data. For most depths, the model's prescriptions avoid the experimental DCS cases, and its prescriptions for 2% probability of DCS are close to those of a deterministic model based on the VVal-18 Algorithm. Our model indicates that the long times at decompression stops mandated by some probabilistic models are not warranted and that these other models' estimates of DCS risk are incorrect. Our model, which cannot be used operationally because it cannot calculate depths and times at decompression stops, indicates that the VVal-18 Algorithm is acceptable for computing the decompression requirements of single-level, non-repetitive air dives.

20. DISTRIBUTION/AVAILABILITY OF ABSTRACT	21. ABSTRACT SECURITY CLASSIFICATION
☐ UNCLASSIFIED/UNLIMITED ☒ SAME AS RPT. ☐ DTIC USERS	Unclassified

22a. NAME OF RESPONSIBLE INDIVIDUAL	22b. TELEPHONE (Include Area Code)	22c. OFFICE SYMBOL
NEDU Librarian	850-230-3100	

DD Form 1473

FOREWORD

This work was supported in part by the Deep Submergence Biomedical Development Program, Naval Sea Systems Command, Task Numbers 63713N S0099 01A 99-04 and 63713N S0099 01A 01-07. The opinions and assertions contained herein are the personal views of the authors and are not to be construed as official or as reflecting the views of the Navy Experimental Diving Unit or the U.S. Navy.

CONTENTS

FIGURES

TABLES

INTRODUCTION

Decompression tables are instructions for bringing divers to the surface without causing them to contract decompression sickness (DCS). A majority of military, commercial, and sport dives are "no-stop" dives. For no-stop dives the decompression tables prescribe a limit to the time that divers can remain underwater if they are to avoid DCS. If they must stay longer than the no-stop time, they follow decompression table instructions for ascent to "decompression stops" at depths part way toward the surface, depths where they remain for times prescribed by the table. The sum of these times that divers spend at decompression stops plus the time required to travel to the surface is the "total decompression time" (TDT).

Most current tables are generated from "deterministic models," which embody an underlying assumption that there is a threshold for development of DCS. Deterministic tables are formulated from intuition and assumptions about the threshold. Diving experience is used informally before the table is generated and to check the final product. In contrast, "probabilistic models" imply that the response to decompression stress is graded, so that even ostensibly safe dives carry a small but finite risk. Probabilistic models are generated by applying statistical techniques to dive-outcome data (information about whether or not a certain dive profile resulted in decompression sickness).[1] Assumptions about risk are incorporated into an equation or algorithm, and parameter values of the equation or algorithm are then estimated by statistically analyzing the dive-outcome data, sometimes called "calibration" or "training" data. We define a probabilistic model as the algorithm with its parameter values. The tolerable risk for a given dive is a matter of policy and may vary according to the circumstances. Discussions at Naval Sea Systems Command (NAVSEA) have resulted in a consensus that more than 2 DCS cases per 100 dives would hurt diver morale and slow operational tempo (personal communication, C. A. Murray; 2000).

"Standard air dives" can be defined as dives to depths of 25 to 190 feet of seawater, gauge (fswg; 1 fsw = 3.063 kPa; 33.08 fswg = 2 atmospheres absolute), inclusive, with bottom times of 720 min or less, where bottom time is defined as the elapsed time from leaving the surface to leaving the bottom depth. A recently published probabilistic model that we will call the "NMRI-98 Model" (model 2) mandates long times at decompression stops for standard air dives.[2] These long TDTs conflict with information abstracted from carefully documented U.S. Navy dive trials[3] and also with information from a deterministic model, the "VVal-18 Algorithm."[4,5] Figure 1 illustrates the discrepancy by comparing model prescriptions with outcome data on a graph similar to those developed in our earlier work.[3] This example is for dives to depths of 150 fswg and with various bottom times. The traces in Figure 1, which show ascent instructions for three

different tables, rise because longer bottom times at the given depth require more decompression stops and longer decompression stops. The trace labeled "USN57" represents the current U.S. Navy Standard Air Table;[6] for example, the TDT for a 60-minute bottom time at 150 fswg is 115 min.

In Figure 1, triangles show particular dive trials to depths between 146 and 150 fswg that resulted in one or occasionally two cases of DCS, and circles show trials in which no DCS occurred in groups of one to 15 divers. Consider the locations of the three table traces relative to the data points in Figure 1:

- Six triangles are above the USN57 trace: this supports previous contentions that the USN57 table does not prescribe sufficient time at decompression stops to avoid DCS.[3,7,8]
- The VVal-18 trace lies above all the triangles: that is, the model instructs divers to spend enough time at decompression stops to avoid the DCS cases shown on the graph. For example, the VVal-18 trace indicates that TDT should be 134 min for a bottom time of 30 min, but TDT was less than 100 min for the divers who participated in the test dives that gave rise to the triangles near the bottom time of 30 min.
- For long TDTs, the trace for the NMRI-98 probabilistic table is far from any circles or triangles. For many bottom times, NMRI-98 prescribes TDTs several times longer than those for the deterministic VVal-18 table.

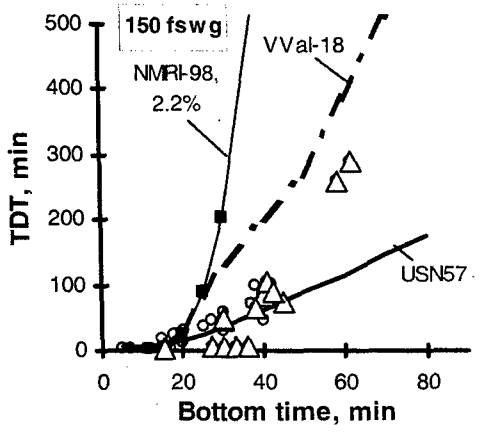

FIGURE 1. Traces for decompression tables (NMRI-98, VVal-18, and USN57), along with points for dive-outcome data. Triangles locate the bottom times and TDTs of particular dive trials that resulted in at least one case of DCS. Circles show trials that produced no DCS in any divers.

The essence of a statistical technique is to fit an equation to data points. However, our previous work shows that the NMRI-98 Model prescribes TDTs that are far longer than TDTs of documented DCS cases for the entire range of standard air dive depths from 40 to 190 fswg.[3] The NMRI-98 calibration data includes saturation dives, which can have TDTs much longer than those for standard air dives. We suggest that including saturation dives in the calibration dataset used with the NMRI-98 Model may have caused it to prescribe excessively long TDTs.[9] An earlier probabilistic model produced at the Naval Medical Research Institute, which we will call the "NMRI-93 Model," also prescribes long times at decompression stops for reasonable DCS risks around 2%.[10]

Our long-term goal is to develop a set of nitrogen-based decompression tables that correct safety and capability deficiencies of current tables. Objectives for the present work are

1) to develop insight about probabilistic models, particularly about the long TDTs that are a feature of previous models;[2,10]
2) to assess whether new air tables generated from the VVal-18 Algorithm[4,5] would be appropriate; and
3) to develop a convenient way to estimate DCS risk for air dives.

Our approach is to produce a relatively simple probabilistic model that can provide probability estimates for any air decompression table.

THE U.S. NAVY DECOMPRESSION DATABASE

The U.S. Navy Decompression Database consists of many computer files, each representing a particular decompression study.[11,12] Within each file the specific test dive profiles are listed sequentially. Each profile entry bears a summary heading that describes the profile and its outcome, followed by a series of lines showing the depth/time nodes of the profile. Figure 2 illustrates a typical entry.

```
 150.0,  73.2,  143.8, DIV361      1 REPETS= 1
1.000,   1, 1.0,  252.0,  312.0,
```

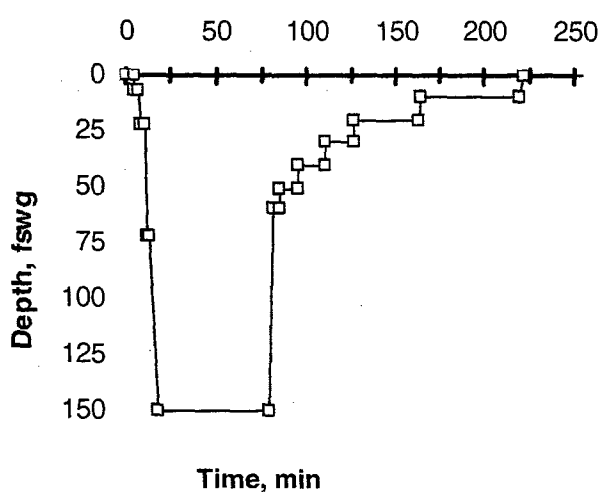

Figure 2. Illustration of the information in the U.S. Navy Decompression Database. The box shows a sample heading for a dive profile from file EDU1180S. The plot of depth below sea level versus time is a graph of the body of the tabular data (not shown here).

The box above the graph shows the heading. The top line shows the dive depth in fswg, the bottom time in min, TDT in min, and, between the last comma and the end of the line, a coded comment about the profile and its relation to other profiles in the same series.

The 1.000 in the second line of the heading signifies the gas breathed before the dive: 1.000 is the code for air. The subsequent 1 indicates the number of person-dives included in this particular profile, and the following 1.0 indicates that this diver suffered DCS. The number here would be zero if no DCS cases had occurred and 0.5 if the DCS had been considered a "marginal" case

— a diagnosed DCS case that was not considered severe enough to require treatment. For the same profile, separate database entries indicate divers who were DCS free, who had marginal DCS, and who had DCS.

The 252.0 in the second line of the heading is T1, the last time (in minutes) since the start of the dive when the diver was surely free of signs or symptoms of DCS. The 312.0 is T2, the first time (in minutes) when signs or symptoms of DCS were noted.

The times and depths plotted in Figure 2 are from the body of the dive-profile information, which follows the heading in the data files. The dive was to 150 fswg, with bottom time of 73.2 min and TDT of 143.8 min, including six decompression stops. The observation period extended beyond the graph to 1,662 min. If the divers breathed a gas mixture other than air during the dive, codes in the profile information indicate the mixture, as well as the times and depths at which the breathing of the non-air mixture commenced and stopped.

METHODS

DIVE-OUTCOME DATASETS

We used Microsoft Excel 97 SR-1 and single-level, nonrepetitive, nitrogen-based experimental dives documented in the U.S. Navy Decompression Database[11,12] to generate a dataset for calibration of our "StandAir" Model (see Table 1). In the Database, a separate report describes each of the 19 source files, each of which contains a series of entries that provide information about one to 86 persons who followed a particular dive profile.

To prepare the calibration dataset, we carefully studied the details of the time and depth profiles of each entry, using the heading of the entry as a guide (see Figure 2). We deleted profiles having more than one distinct bottom depth or an indistinct series of bottom depths. When the recorded information in a profile indicated that the heading was inaccurate or that a small deviation from a square-wave exposure to depth occurred, we made appropriate corrections so that the corrected depth, bottom time, and TDT pattern corresponded approximately to square-wave behavior. Delays at the beginning and end of the dives necessitated by far the most corrections, and datafiles DC4D, DC4W, and EDU885A needed the most corrections. We made corrections in 311 profiles representing 1,051 person-dives; there were150 person-dive corrections for depth (average absolute change = 1.59 fswg), 732 for bottom time (average absolute change = 3.74 min), and 474 for TDT (average absolute change = 2.49 min).

TABLE 1. STANDAIR CALIBRATION DATASET: DETAILS OF SOURCE FILES

(1)	(2)	(3)	(4)	(5)	(6)	(7)	(8)	(9)	(10)
	Source file	Date	Entries	Person -dives	Cases Obs	Cases Pred	% Obs	% Pred	Chi-square
1	DC4D	10/9/97	247	775	19	17.4	2.5%	2.2%	0.15
2	DC4W	12/21/93	141	240	8	6.7	3.3%	2.8%	0.25
3	EDU1157	9/23/97	27	46	15	17.7	32.6%	38.5%	0.41
4	EDU1351NL	12/3/96	43	143	2	3.9	1.4%	2.7%	0.93
5	EDU159AVL	9/30/97	5	11	5	1.1	45.5%	10.0%	13.83
6	EDU545	11/20/97	42	94	18	10.8	19.1%	11.5%	4.80
7	EDU557	5/29/97	135	568	27	51.6	4.8%	9.1%	11.73
8	EDU849LT2	5/5/97	74	141	26	15.8	18.4%	11.2%	6.58
9	EDU849S2	6/27/97	35	60	13	13	21.7%	21.7%	0.00
10	EDU885A	12/20/93	82	483	30	24.1	6.2%	5.0%	1.44
11	EDUAS45	1/15/98	10	14	3	2.3	21.4%	16.4%	0.21
12	NMR8697	1/29/91	229	477	11	13.9	2.3%	2.9%	0.61
13	NMR97NOD	8/19/97	9	103	3	2.6	2.9%	2.5%	0.06
14	NMRNSW	1/29/91	43	86	5	4.5	5.8%	5.2%	0.06
15	NSM6HR	12/20/93	19	57	3	2.3	5.3%	4.0%	0.21
16	PASA	5/26/92	26	72	5	2.5	6.9%	3.5%	2.50
17	RNPL52BL	7/20/95	27	192	1	6.9	0.5%	3.6%	5.04
18	RNPL57L	7/21/95	50	50	9	3.2	18.0%	6.4%	10.51
19	RNPLX50	9/19/97	16	57	5	7.6	8.8%	13.3%	0.89
	Totals		1,260	3,669	208	207.9 **± 57.9***			60.2

* 95% confidence interval

1) We took the bottom time to be the difference between the time when divers left a depth of 3 fswg or shallower and the time when they left the bottom depth. All profiles of EDU885A needed correction for lags at 7 fswg at the beginning of the dives, with an average correction of −2.54 min ± 1.34 min standard deviation (SD).

2) We took the TDT to be the difference between the time when divers left the bottom depth and the time when they reached a depth of 3 fswg or shallower. We verified that the pattern of decompression stops in the test dives was generally in line with Navy practice: the stops began at depths that were relatively shallow compared to the bottom depth and stop times lengthened at successive stops (for example, see Figure 2).

3) We adjusted for irregularities in the depth so that the area under a graph of depth vs. bottom time was approximately equal to the area under an uncorrected graph:

   - When the summary heading did not account for a delay near the final bottom depth, we made the bottom depth less.
   - When the summary heading did not account for a slow descent to depth, we shortened bottom time and/or decreased bottom depth.
   - When the summary heading did not account for small variations in bottom depth, we took average depth.

We considered marginal cases, defined as "transient aches or pains following a dive that seem related to the pressure exposure, but were not of a severity or persistence to warrant treatment,"[13] to be non-cases.

The EDU159AVL file (Table 1, row 5) contains information on 11 person-dives to 34, 36, and 38 fswg; we changed the information from that in the U.S. Navy Decompression Database file, EDU159A, following our rereading of the original documentation of the dives.[14]

The StandAir dataset contains 1,260 entries, 3,669 person-dives, and 208 DCS cases. Forty-five percent of the person-dives are no-stop dives, or nearly so, on the basis that their TDT is less than 1.5 times that expected for an ascent rate of 30 fsw/min; average depth for these is 92 fswg. For 515 of the no-stop dives with 11 DCS cases, the breathing gas at depth was a nitrogen mixture with inspired oxygen fraction (FO_2) different from that of air (0.21). For these we calculated an equivalent air depth (EAD) in fswg to replace the actual depth (D) in fswg:

$$EAD = \left(\frac{1 - FO_2}{0.79} \right) \cdot (D + 33) - 33 \qquad (1)$$

The StandAir dataset does not include saturation dives, repetitive dives, or multilevel dives. Bottom times are 5 to 720 min inclusive, average 98 min; depths (or air-equivalent depths) are 28 to 300 fswg inclusive, average 118 fswg; and TDTs are 0.6 to 1,445 min inclusive, average 43 min. Many ascent rates are 60 fsw/min, whereas the rate currently prescribed for the U.S. Navy is 30 fsw/min.[6] The Cases Pred and % Pred columns in Table 1 preview the statistical fit covered in the **RESULTS** section.

DISTRIBUTIONS OF VARIABLES IN THE CALIBRATION DATASET

Figure 3 illustrates the distributions of variables in our calibration data. A statistical model is most reliable in regions that have the most data points. The histograms in Figure 3 show that the reliability of the StandAir Model will be low for bottom times greater than 79 min and for dives with TDTs longer than 20 min. Fortunately the bulk of the calibration data is in the low-incidence region, which is of interest for operational diving: for 80% of the person-dives, incidence of DCS estimated by the StandAir Model is below 3%; for 63%, below 2%; and for 47%, below 1%.

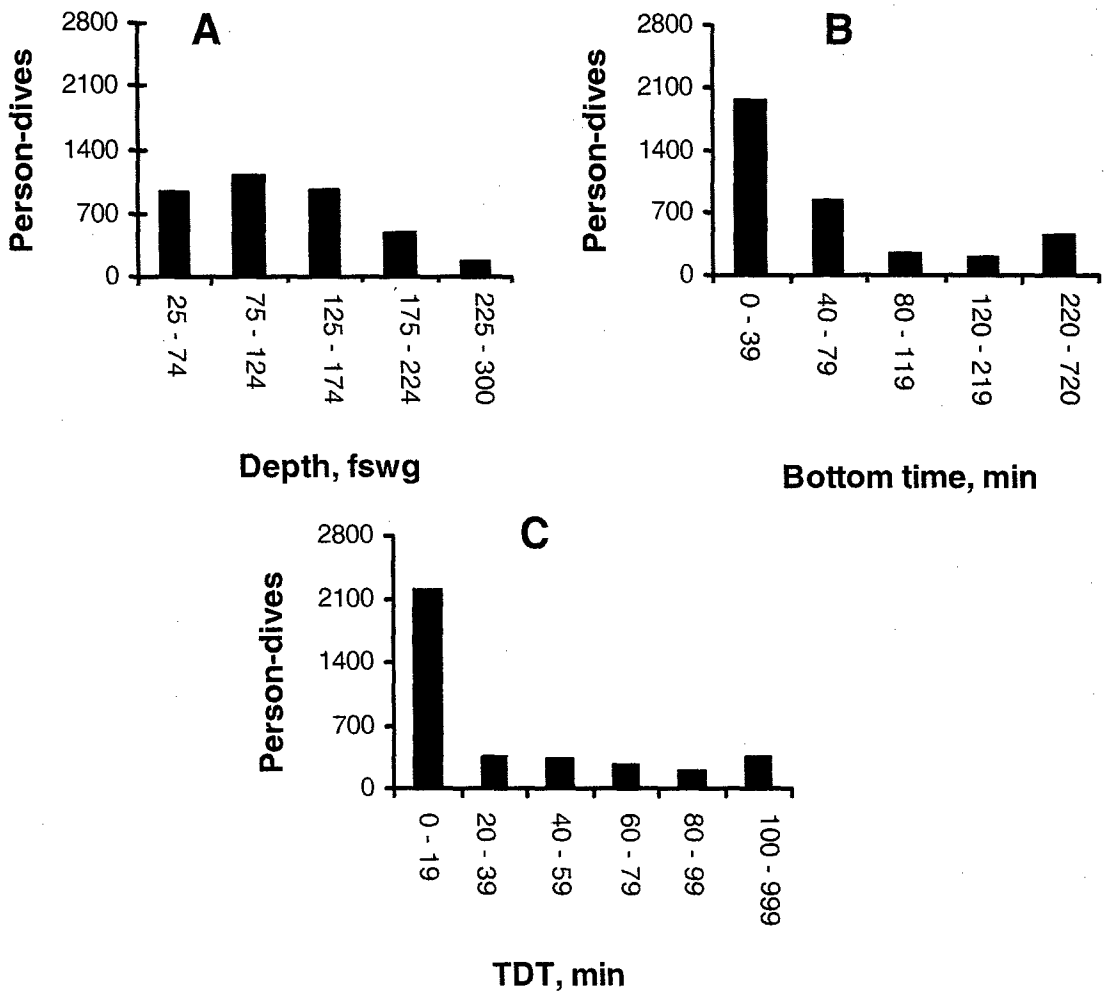

FIGURE 3. Histograms of the StandAir calibration data. Each panel includes data from 3,669 person-dives.

STATISTICAL ANALYSIS

For maximum likelihood estimation of parameters, the NONLIN module of a commercial statistical program, SYSTAT,[15] uses a *LOSS* function, an alternative to least squares of residuals. The log-likelihood (*LL*) is specified as the negative of the *LOSS* value. Equation 2 gives the *LOSS* statement for a single entry of dive-outcome data in the dataset; the *LOSS* function is the sum of all *LOSS* statements for all entries of the dataset.

$$LOSS = -DIVES \cdot [DCS \cdot ln\,(ESTIMATE) + noDCS \cdot ln\,(1 - ESTIMATE)] \qquad (2)$$

DIVES is the number of person-dives in the group test that makes up the entry, *DCS* indicates whether subjects in the group had DCS, *ln* signifies natural logarithms, *ESTIMATE* is the estimated probability of DCS (*Pdcs*), and *noDCS* indicates that no subjects in the group had DCS. The *DCS* variable is either a 1 or a zero, because divers who dived together and did not contract DCS (up to 86 divers in a profile) are listed together in the same profile entry in the database (*DCS* = 0), but divers who contracted DCS are listed separately (*DIVES* = 1, *DCS* = 1). Parameter estimation minimizes the positive *LOSS* function, which is the same as maximizing the negative *LL*, by a quasi-Newton technique that uses numeric estimates of the first and second derivatives of the *LOSS* function to seek a minimum. In addition to estimating parameters, the NONLIN module computes asymptotic standard errors (*ASE*) and the asymptotic correlation matrix by estimating the Hessian matrix after iterations have stopped.

We chose the logistic regression paradigm to characterize probability:

$$Pdcs = \frac{1}{1+e^{(-LOGIT)}} \qquad (3)$$

$$LOGIT = a + b \cdot (D - c) \cdot \left(\frac{1 - e^{\left(-d \cdot T^{f}\right)}}{TDT - g} \right) \qquad (4)$$

Equation 4 is the particular *LOGIT* function we used for our StandAir Model; a rationale appears in the Discussion section. Symbol *D* represents dive depth in fswg; *T*, bottom time in min; *TDT*, total decompression time in min; and *a*, *b*, *c*, *d*, *f*, and *g*, parameters estimated by the logistic regression process.

Three kinds of confidence intervals are of interest:

1) We use the binomial theorem to calculate confidence intervals for the "true" incidence of DCS in the entire population from a limited sample of person-dives.
2) We calculate confidence intervals for the probability estimates of the model from the parameters, *ASE* values, and the asymptotic correlation matrix as outlined by Ku.[16]
3) Confidence intervals for estimated parameters are calculated by the SYSTAT program.

Once the parameters of Equation 4 are found by statistical analysis, *Pdcs* can be tabulated for *D*, *T*, and *TDT* of each entry in the calibration dataset. To find *TDT* for particular combnations of *D*, *T*, and *Pdcs*, a specially designed computer program calculates *Pdcs* over ranges of *D*, *T*, and *TDT* by solving Equation 3 for a run of depths and, within each depth, for a run of bottom times, and within each bottom time, for a run of TDTs. The program writes the depth, bottom time, *TDT*, *Pdcs*, and confidence interval to a file when the *Pdcs* just exceeds a predetermined target, and the program then continues to the next bottom time and eventually to the next depth.

We used the Microsoft Excel spreadsheet program to generate least-squares trend lines and curves. We performed chi-square tests to assess whether differences between observed DCS cases and cases predicted by the model are greater than expected from chance:

$$\chi^2 = \Sigma [(Co - Cp)^2 / Cp] \qquad (5)$$

In Equation 5, *Co* is the number of cases observed in some subset of the data, and *Cp* is the number of cases predicted in the subset. Small values of the calculated χ^2 value indicate that the model is a good fit to the calibration data.

EVALUATION USING INDIVIDUAL POINTS

The statistical evaluation is essentially a data-smoothing process that establishes a probabilistic model's parameters from the entire calibration dataset. After the model was developed, we used the calibration data a second time by observing how the individual points in the dataset corresponded to the instructions for ascent. As in Figure 1, the trace of a table on a bottom-time/TDT plot is compared with the locations of circles (divers free of DCS) and triangles (DCS cases). A triangle below the table trace is expected, because the diver has spent

less time at decompression stops than the table instructs him to spend. Having more than a few triangles above a table trace indicates that the table lacks sufficient TDT to prevent DCS. Triangles can appear anywhere below the table trace, depending on the bottom time and TDT of the dive, but a table that prescribes 1% incidence theoretically has less than one triangle above the trace for every 100 person-dives. Circles can appear both below and above the trace, because high-risk dives can sometimes result in zero DCS by chance.

Because the dive-outcome data in the StandAir dataset span a continuum of depths and bottom times, we are unable to limit the outcome data to the specific depth of a graph. Instead, we compare table traces with DCS cases for dives that are 0 to 5 fswg (white triangles) shallower and 6 to 10 fswg (gray triangles) shallower than the depth for the table trace. Finally, small circles on the plots signify dives that did not produce DCS at depths as much as 10 fswg shallower than those of the table traces. For example, for graphs showing table traces for 60 fswg, we would plot white triangles for DCS cases that occurred with dives to depths of 56 through 60 fswg, gray triangles for cases that occurred with dives to 51 through 55 fswg, and small circles for DCS-free dives to 51 through 60 fswg. Note that the gray triangles should be farthest from the trace for table instructions. A gray triangle to the left of a trace, above it, or close to it is stronger evidence of a table's inadequacy than is a white triangle in the same position. Because laws of chance predict very few white triangles above the trace of a good table, the trace serves essentially as an upper limit, and the uppermost triangles on a plot of TDT versus bottom time are the key to evaluating a table trace. The upper limit for gray triangles is expected to be below the upper limit for white triangles, because the depths for the gray-triangle DCS cases are shallower than those for white-triangle cases. For 6 DCS cases among 236 dives that used a breathing gas having a fraction of O_2 less than that of air (0.21), we drew a large circle around the triangle on the graph. For 5 DCS cases among 279 dives that used a fraction of O_2 greater than that of air, we drew a large square around the triangle.

RESULTS

MODEL RESULTS

Table 2 lists the parameters estimated by fitting Equations 3 and 4 to the calibration dataset. The *LL* value is considerably better than the *LL* for the null model, in which *Pdcs* equals the DCS incidence in the dataset. As judged by the high ratios of model parameters to their asymptotic standard errors (Param/*ASE*), the parameters are tightly estimated. The correlation matrix for the StandAir Model shows high correlation between parameters *c* and *d*. As seen in Table 1, the StandAir Model predicts all 208 cases in the StandAir calibration data. The

TABLE 2. PARAMETERS FOR THE STANDAIR MODEL

$$LOGIT = a + b \cdot (D - c) \cdot \left(\frac{1 - e^{(-d \cdot T^f)}}{TDT - g} \right)$$

LL = –669.144 (Null model, *LL* = –798.978, inc = 5.67%)

Parameter	Estimate	*ASE**	Param/*ASE*	Wald 95% Confidence Interval
a	-6.022169	0.277405	-21.7	-6.57 – -5.48
b	86.596315	18.887942	4.58	49.5 – 123.6
c	25.091718	2.038656	12.31	21.09 – 29.09
d	0.002929	0.000832	3.52	0.0013 – 0.0046
f	0.918547	0.041705	22.0	0.837 – 1.000
g	-170.304442	21.500126	-7.92	-212 – -128

Correlation matrix

	a	*b*	*c*	*D*	*f*	*g*
a	1.000					
b	0.132158	1.000				
c	0.427921	0.417632	1.000			
d	-0.569450	-0.541532	-0.92333	1.000		
f	0.330143	-0.453320	0.503751	-0.458797	1.000	
g	0.074836	-0.075632	0.739574	-0.580370	0.590638	1.000

*ASE = asymptotic standard error

largest differences between observed and predicted incidences are for files EDU159AVL, RNPL57L, EDU557, and EDU849LT2. Chi-square for the DCS cases in Table 1 is 60.2, as opposed to the tabulated value of 30.1 for 95% confidence and 19 degrees of freedom. Thus there is considerable probability that the differences between observed and predicted cases are not due to chance alone.

Many sources of variability cause uncertainty in probabilistic models — differences between the dives in different test settings (e.g., wet vs. dry dives, exercising vs. sedentary subjects, warm vs. cool temperatures, etc.), differences in DCS criteria with different investigators, and changes in dive practice over the years. The dark bars in Figure 4 illustrate the uncertainty of the parameters that underlie our StandAir Model: the vertical standard error line segments are a large percentage of the value for parameters *b* and *d*. The white bars show parameters of an unpublished model based on Equation 4, a model that used the uncorrected entry headings of the files in the StandAir calibration dataset. Corrections to the headings caused little change in the parameters; for both models, the small errors that we corrected in the profile headings contributed to an overall uncertainty that is small compared to other sources of uncertainty. There is little reason to prefer one model shown in Figure 4 over the other.

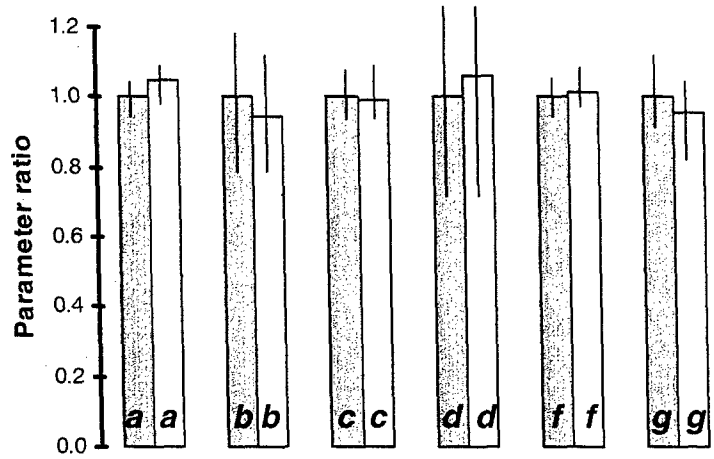

Figure 4. Uncertainty of the parameters of the StandAir Model (dark bars, normalized); vertical line segments show plus and minus one asymptotic standard error, normalized to the parameter value. White bars show parameters and errors of a model based on uncorrected headings of the database files.

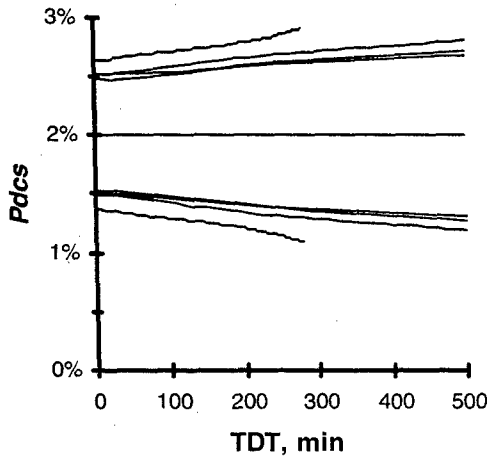

FIGURE 5. Upper and lower 95% confidence intervals for various depths as a function of TDT for the StandAir Model evaluated for 2% *Pdcs* (central straight line = 2% *Pdcs*). From the outer to the inner traces: 40, 60, 100, and 180 fswg.

Figure 5 shows confidence intervals around *Pdcs* of 2% plotted as a function of TDT to illustrate the uncertainty associated with our model. As TDT increases, the distances between upper and lower traces increase modestly and are as great as 1.8%. When estimated *Pdcs* is 2%, the true *Pdcs* could actually be somewhere between 1.1 and 2.9%. For all *Pdcs* values of interest, the average width of the confidence intervals for the StandAir Model is about 60% as large as the *Pdcs.* The average interval in Figure 5 is about 1.2%; it would be about 3% when *Pdcs* = 5%, and about 6% when *Pdcs* = 10%.

PREDICTIONS VERSUS OBSERVATIONS FOR GROUPED DATA

Figure 6 compares estimates from the StandAir Model with observed outcomes. To produce the graphs, we sorted the entire dataset by a particular variable and then divided the sorted set into seven bins of approximately equal numbers of person-dives. For optimizing parameters, it would be preferable to have the DCS cases spread equitably with regard to depth, bottom time, and TDT, so that each of the bins has equal numbers of DCS cases. In Figure 6A the left-hand bin shows slightly more than 6 observed DCS cases per 100 dives, and the numbers vary in the other bins. The DCS incidence is high for long TDTs (Figure 6B) and long bottom times (Figure 6C). In all cases, predicted values follow the observed values closely. The enlargement of the short bottom-time range in Figure 6D shows the only case in which the predicted incidence is outside the confidence interval for the observed incidence. Chi-square values for the plots in Figure 6 are 3.2 for depth, 11.0 for bottom time, and 8.0 for TDT. Degrees of freedom for

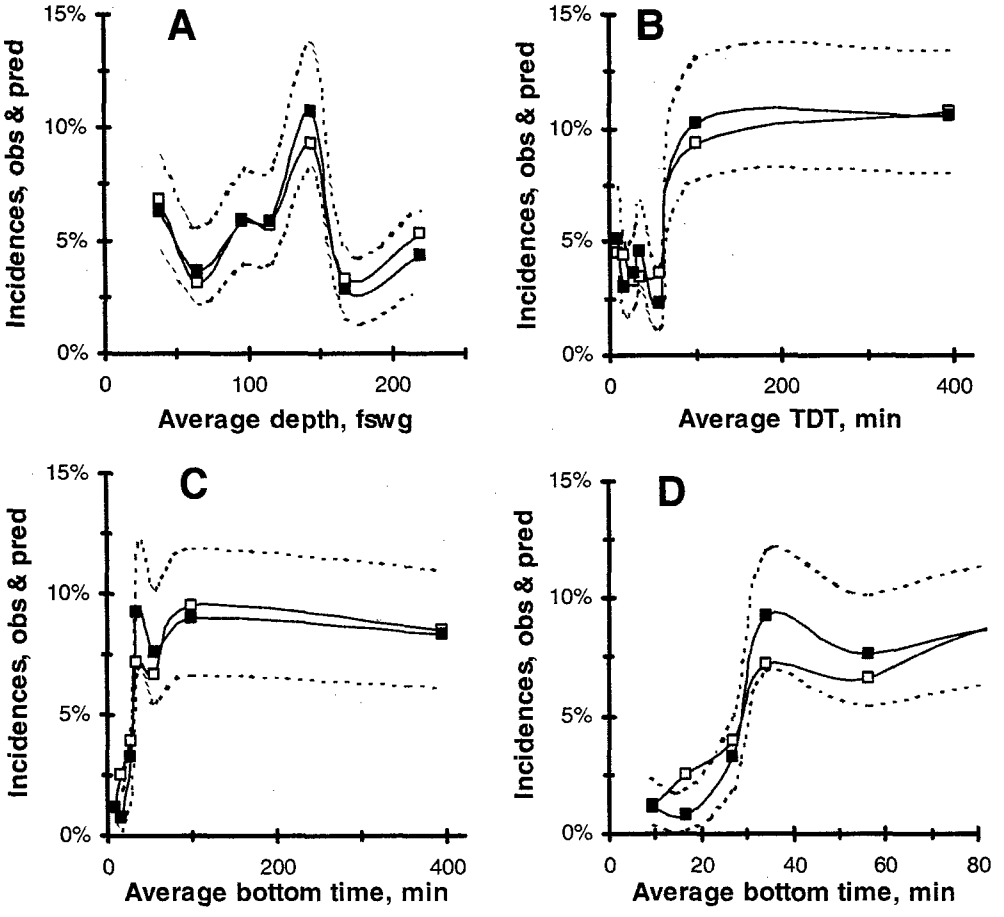

FIGURE 6. Incidences (DCS cases per 100 person-dives) as functions of a variable for subdivisions of the data containing equal numbers of person-dives. Filled rectangles = observations; open rectangles = predictions. Dotted curves show 95% confidence intervals, calculated by the binomial theorem, around observed incidences. A: incidences versus depth. B: same format, but for TDT. C: same format, for bottom time. D: short bottom times.

each of the plots are 6, since there are 7 bins. The chi-square table lists 12.6 for 95% confidence, so none of the differences is greater than any expected by chance if the observed and predicted DCS cases are from the same population.

Figure 7A shows observed versus predicted incidence. The values for the X-axis are obtained by calculating *Pdcs* for each row in the StandAir calibration dataset, sorting according to estimated *Pdcs*, and then dividing the sorted data into bins having approximately the same number of person-dives. The numbers of DCS cases predicted by the StandAir Model for each bin are then added up. The values for the Y-axis are obtained by counting the number of DCS cases observed among the dives in each bin.

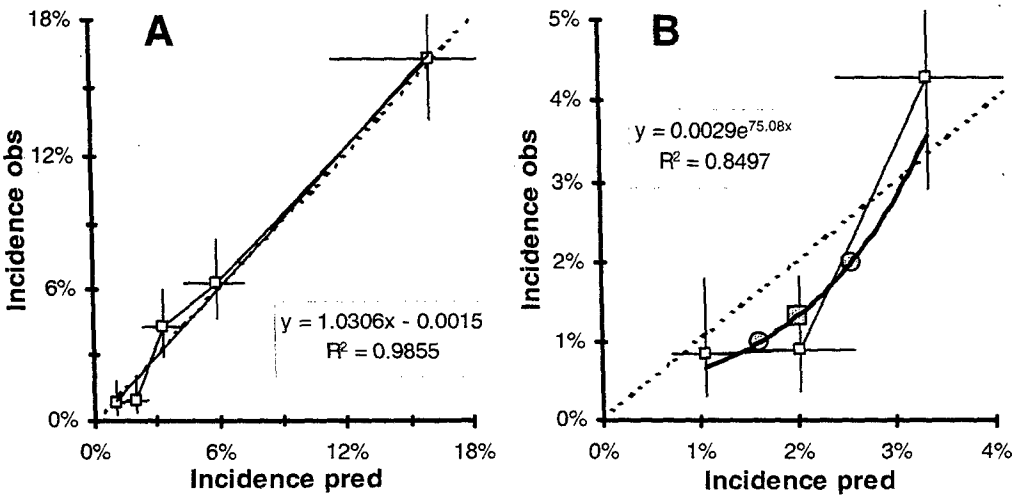

FIGURE 7. A: Observed incidence of DCS is plotted against incidence predicted by the StandAir Model. Dotted 45° line = identity; solid line is the least-squares line through all the points; correlation coefficient and the equation for the line are shown in the box; vertical and horizontal lines show 95% confidence intervals around observed and predicted incidences. B: Low-incidence region of Panel A is shown. The heavy curve is a least-squares trend curve through the three data points (see box); gray circles are located at an observed incidence of 1.0% and predicted incidence of 1.63% and at an observed incidence of 2.0% and a predicted incidence of 2.56%. A gray square is at an observed incidence of 1.3% and a predicted incidence of 2%.

The data points in Figure 7A approximate a straight line but are slightly above the dotted identity line for most of its extent and below it at the extreme left. A least-squares trend line (see equation) is essentially superimposed on the identity line. Except for the point furthest to the right, the horizontal lines for uncertainty in predicted incidence are shorter than the vertical lines for uncertainty in observed incidence. The chi-square value for the DCS cases represented by the points in Figure 7A is 7.52, and the tabulated chi-square is 9.5 for 95% confidence and 4 degrees of freedom. The differences between observed and predicted DCS cases could be due to chance. The chi-square value for the cases represented by the three data points in Figure 7B is 7.28, and the tabulated chi-square is 5.99 for 95% confidence and 2 degrees of freedom.

Figure 7B, the low-incidence region of Figure 7A, shows that observed incidence is a little lower than predicted incidence in the operationally important low-incidence region below 3% *Pdcs*. The gray square illustrates that when the data are smoothed by a least-squares process, the model predicts an incidence higher than is actually observed: the observed incidence is only 1.33% when the predicted incidence is 2%. Similarly, the left-hand gray circle shows that when the observed incidence is 1%, the predicted incidence is greater: 1.63%. The right-hand gray circle shows that a 2% observed incidence is associated with a 2.56% predicted incidence. The discrepancy is less for a 3% incidence: a 3.0% observed incidence is associated with a 3.1% predicted incidence. Elsewhere we introduced the idea of adjusting or fine-tuning probabilistic models in the low-incidence region to make them as practical as possible for operational use.[17] For operational dives with a desired incidence around 1 or 2%, our StandAir Model apparently overestimates the risk by about 0.6%, as shown by the gray circles. Thus, the heavy least-squares trend curve and gray points in Figure 5B introduce an important question: which is the more accurate estimate of risk for a particular dive profile — the *Pdcs* calculated by the model, or the observed incidence estimated by a least-squares trend curve through smoothed data?

PREDICTION VERSUS OBSERVATION FOR INDIVIDUAL POINTS

Figure 8A adds a 2% *Pdcs* trace based on parameters for our StandAir Model from Table 2 to the NMRI-98 and VVal-18 traces introduced in Figure 1. The 2% *Pdcs* trace is above all the triangles. The NMRI-98 trace for 2.2% *Pdcs* is below the 2% StandAir trace for short bottom times but is far above it for long bottom times. Figure 8B adds 95% confidence intervals around the StandAir 2% *Pdcs* trace; the confidence interval is wide but does not include the NMRI-98 trace for long bottom times. Figure 8C emphasizes the aberrance of the NMRI-98 trace by repeating the information from Figure 8A on larger scales, along with a trace for 1% by the StandAir Model. At the right of the figure, the NMRI-98 trace has far longer TDTs than do any of the DCS cases and the StandAir and VVal-18 traces. The NMRI-98 point furthest to the right has a TDT that is almost three times greater than that for the 2% StandAir trace.

Figure 8D shows the variation of TDT with variation of *Pdcs*. The TDTs for the 1% trace are roughly twice as long as those for the 2% trace. According to the trend curve in Figure 7B, the *Pdcs* trace for 1.6% matches the observed incidence of 1.0%, the *Pdcs* trace for 2.6% matches the observed incidence of 2.0%, and the *Pdcs* trace for 3.0% is approximately correct for the observed incidence. Thus, the estimates from the trend curve of Figure 7 suggest that the TDTs prescribed by the *Pdcs* isopleths in Figure 8 are longer than necessary to give the stated risk of DCS.

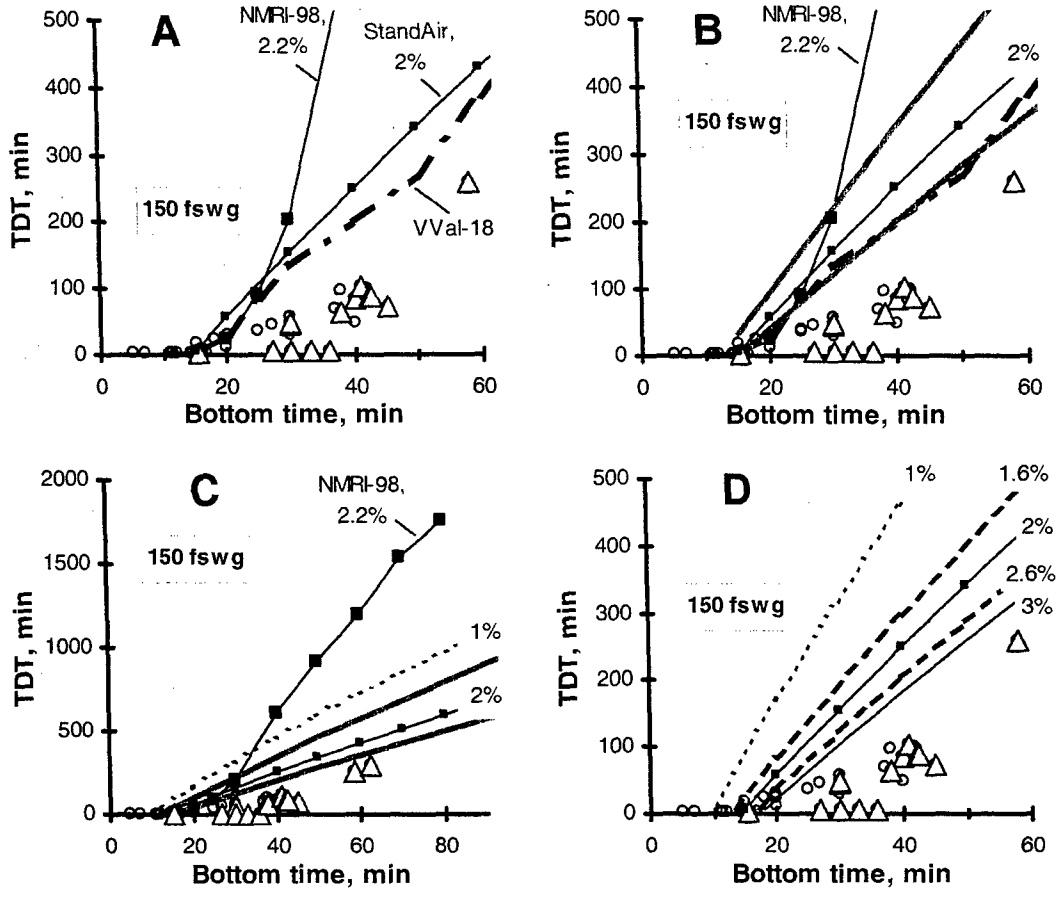

FIGURE 8. Table traces for the StandAir Model. A: This reproduction of Figure 1 adds a trace for 2% *Pdcs*, according to the StandAir Model. B: Heavy gray traces show the 95% confidence intervals for the 2% *Pdcs* trace of Panel A. C: Information from panel B is repeated with a larger scale for TDT. D: Traces for 1.0, 1.6, 2.0, 2.6, and 3.0% *Pdcs*.

The same can be said for Figures 9 and 10. The pattern of the relationship between DCS cases and *Pdcs* isopleths seen at 150 fswg in Figure 8 is typical for the whole range of depths for standard air diving. Figure 9 includes 16 graphs, one for each depth from 40 to 190 fswg, inclusive, at 10 fswg intervals. The dot-dash traces are for the deterministic VVal-18 Algorithm.[4,5] The other traces are for *Pdcs* of 1, 2, and 3%, according to the StandAir Model. The 2.0% *Pdcs* trace is associated with observed incidence of 1.3% (see **PREDICTIONS VERSUS OBSERVATIONS FOR GROUPED DATA**). Similarly, the 1% trace corresponds to observed incidence of less than 1.0%, and the 3% trace corresponds to slightly less than 3.0% observed incidence. Each of the 1,260 entries in the StandAir dataset affords a possibility for a data symbol, a small circle or a triangle, but not all appear because we scaled the graphs to show regions where dive-outcome symbols are near the table traces. Also, many symbols are obscured by other symbols. Figure 10 shows details of short-TDT regions for 12 graphs from Figure 9. Note that the symbols in Figures 9 and 10 show individual data entries from the U.S. Navy Decompression Database[11,12] rather than the combinations of entries that were the basis of our previous work.[3]

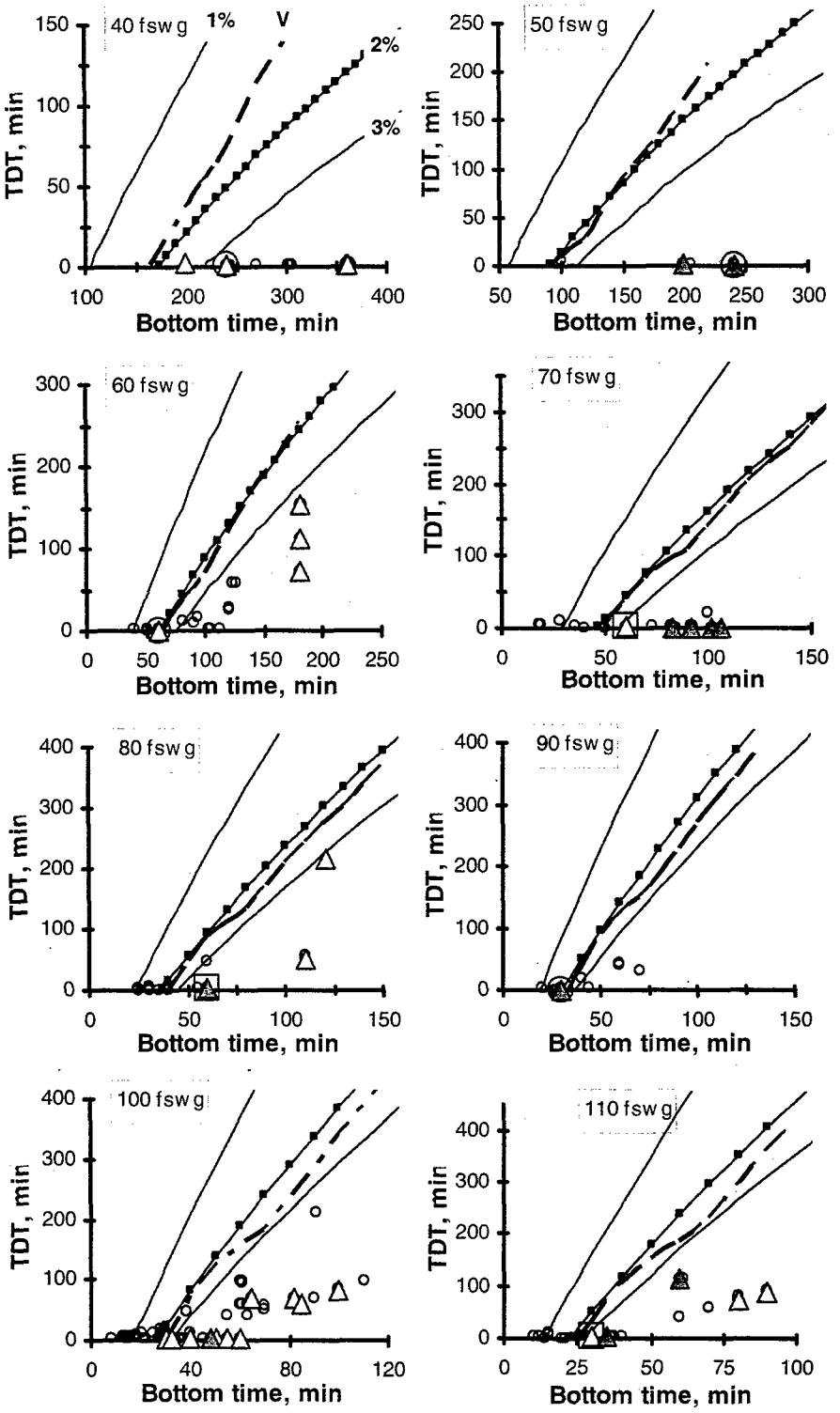

FIGURE 9. First group of depths for evaluation. Traces are for VVal-18 (heavy dashes) and for the StandAir Model for 1% *Pdcs* (left-hand, solid trace), 2% *Pdcs* (middle, solid trace with nodes that indicate individual dive profiles), and 3% *Pdcs* (right-hand, solid trace). Small circles = at least one, or usually many, person-dives without DCS. Triangles = one, or very few, cases of DCS. White triangles = dives less than 5 fswg shallower than the depth indicated on the graph. Gray triangles = dives between 5 and 10 fswg shallower than the depth for the graph.

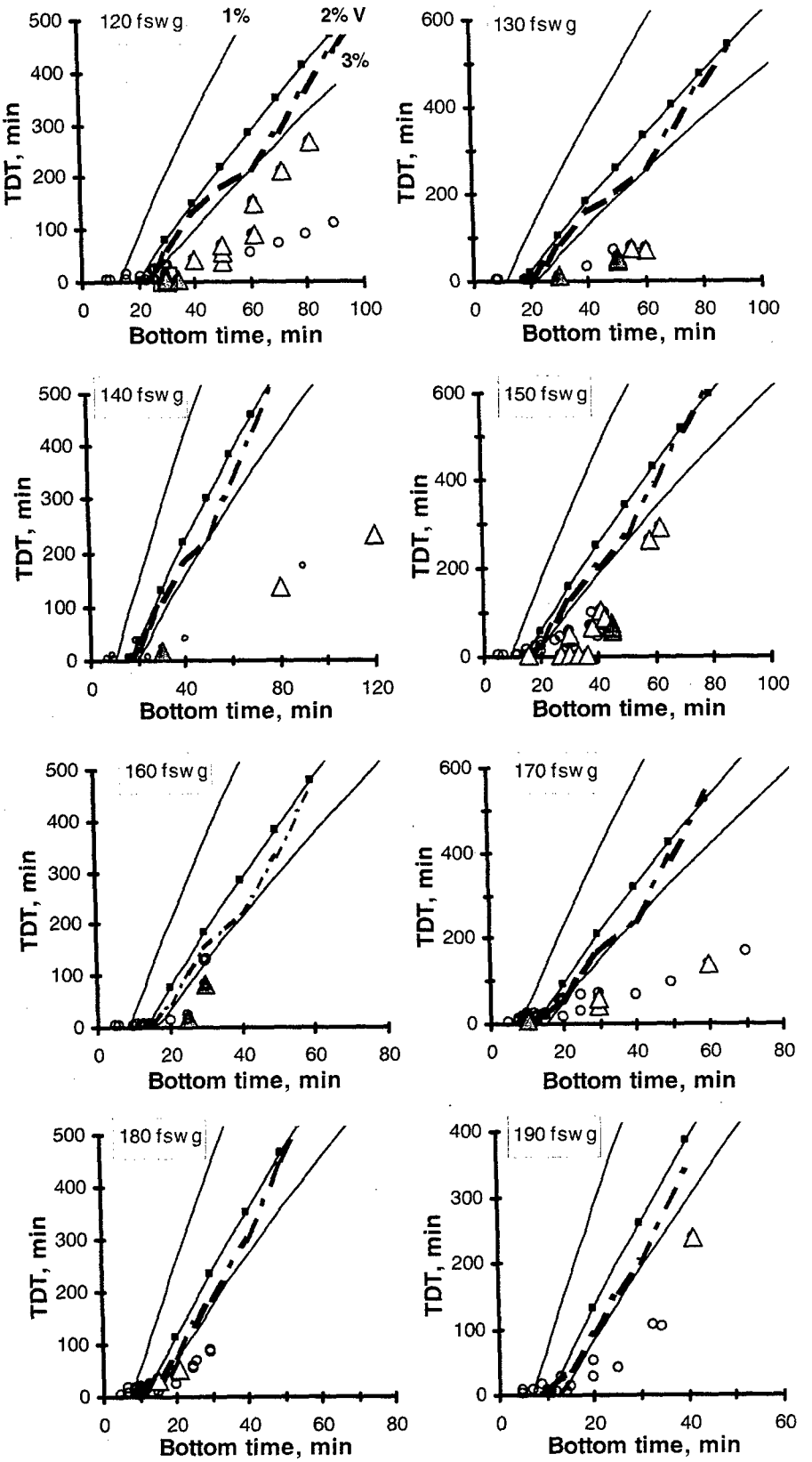

FIGURE 9, CONTINUED. Second group of depths for evaluation.

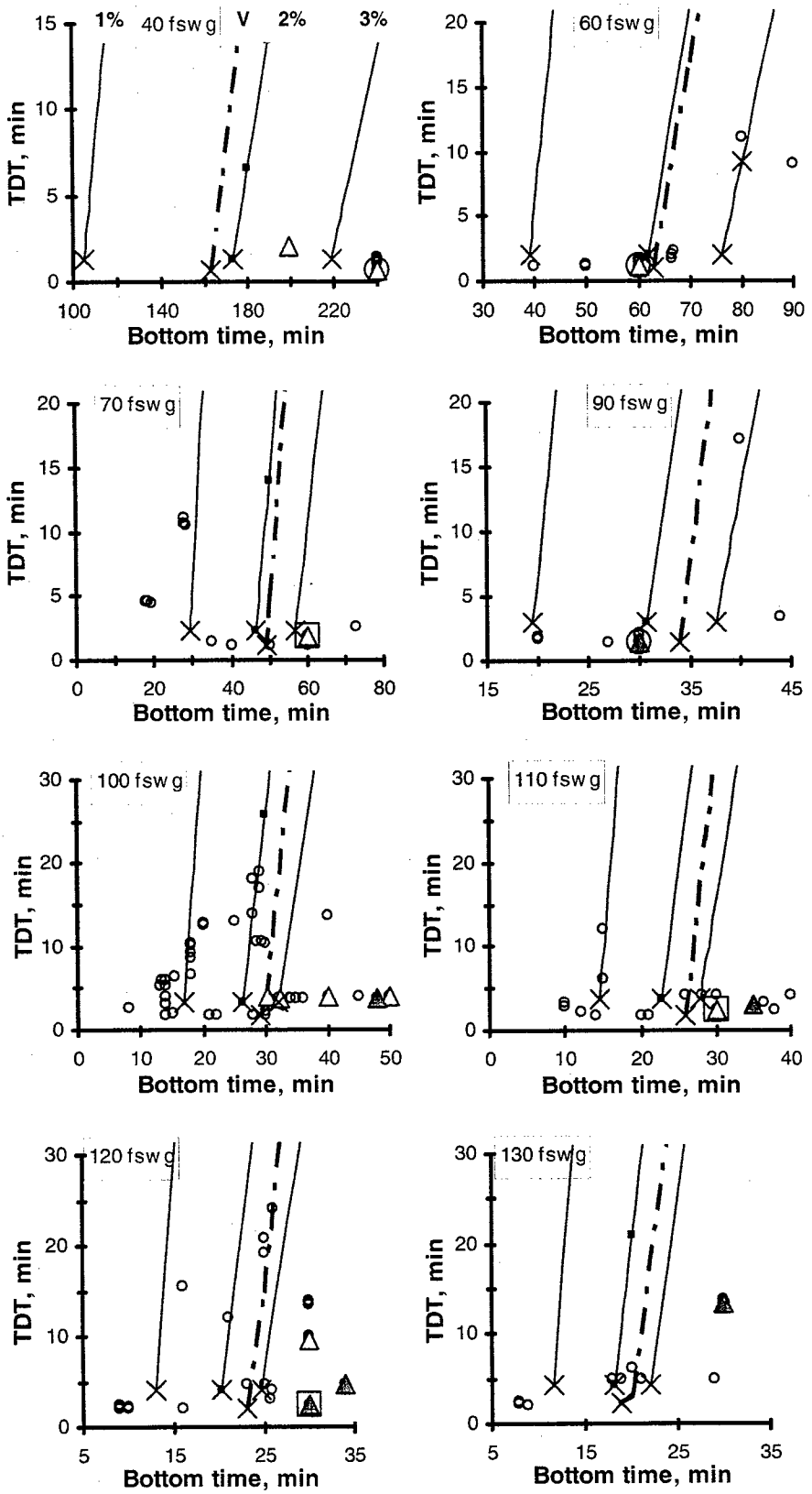

FIGURE 10. First group of depths for short-TDT graphs, with the same format as for Figure 9. As in Figure 9, solid traces (left to right) show 1%, 2% (with nodes), and 3% *Pdcs*; X symbols show no-stop dive points.

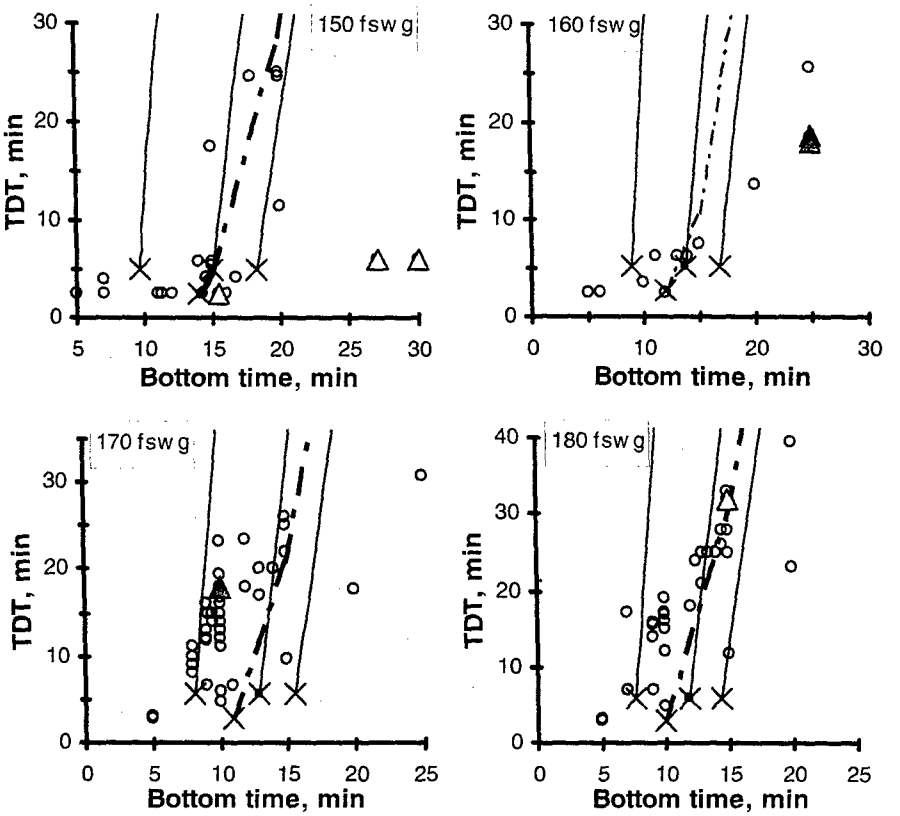

FIGURE 10, CONTINUED. Second group of depths for short-TDT graphs.

The dive-outcome information is scarce, and large uncertainties characterize *Pdcs*, as illustrated in Figure 5, so statements about the VVal-18 Algorithm and our probabilistic model, and especially about TDT prescriptions, cannot be as strong as might be desired — especially for dives with long TDTs.

Comparisons of the positions of the dive-outcome symbols with the table traces in Figures 9 and 10 invite several contentions:

1. The traces for 1, 2, and 3% *Pdcs* span a wide range of TDT for any given bottom time, and, with the exception of the 40 and 70 fswg graphs, the StandAir traces for 2% and 3% *Pdcs* are close to the VVal-18 traces.

2. Several graphs have regions with circles to the left of the 2% *Pdcs* trace and triangles to the right, but these regions occur only at short TDTs (see 100 fswg, for example). For a satisfying evaluation, we would want circles to the left and triangles to the right of the table traces at both long and short TDTs.

3. When the dive-outcome triangles are in regions with relatively long TDT, they are not far below the table traces for 3% *Pdcs* (in Figure 9, see 60, 80, 110, 120, 150, 160, and 190 fswg). This result suggests that the prescribed TDTs for these dives are not too long.

4. Triangles above the table traces would strongly suggest that the prescribed TDTs are too short. Except for those points at very short TDTs in Figure 10, no dive-outcome points, neither circles nor triangles, are above the table traces: therefore, this evaluation yields no definite answer to the question of whether the StandAir Model prescribes TDTs that are too short.

5. A gray triangle near a table trace indicates a more serious risk of DCS than a white triangle in the same position. In Figure 9, gray triangles near traces are on graphs for 80, 90, 110, 120, 130, 140, 160, and 170 fswg. The gray triangle for 170 fswg will be discussed below.

Dives with short TDT and no-stop dives — Figure 10

1. All triangles that suggest inadequacies in the model occur at short TDTs (Figure 10): they are to the left of, or are superimposed on, the 2% *Pdcs* traces. The longest TDTs among such triangles are for an 18-minute TDT at 170 fswg (gray triangle).

2. At short TDT in Figure 10, a few triangles are to the left of, or are superimposed on, the 2% *Pdcs* traces: see 60, 90, and 170 fswg.

3. Of the triangles near the table traces when TDT is short, four (60, 70, 90, and 110 fswg) are for non-air breathing gases. The whole StandAir dataset includes 208 DCS cases, 11 for non-air breathing gas. The overall ratio is 208/3,698 = 0.056, whereas the ratio for non-air breathing mixtures is 11/515 = 0.021. Despite the low ratio of DCS cases per person-dive for non-air mixtures, the non-air dives account for a disproportionate number of the dives that put the safety of the tables in question. In another report we explain our suspicion that non-air dives may be anomalous.[18]

4. At short TDT in Figure 10, a few triangles are between the 2% and 3% *Pdcs* traces or near the 3% traces: see 40, 100 (at 30 min bottom time, 3 min TDT), and 180 fswg.

5. In Figure 10 a gray triangle, which indicates more serious risk than a white triangle, is near the 1% *Pdcs* trace for 170 fswg (165 fswg, 10 min bottom time, 18 min TDT, 2 DCS cases). This gray triangle, plus the white triangles near the 2% *Pdcs* trace on the 150 fswg graph (146 fswg, 16 min bottom time, 2.5 min TDT, 1 DCS case) and180 fswg

graph (172 fswg, 15 min bottom time, 32 min TDT, 1 DCS case) suggest that bottom times are too long for these dives, all of which have short TDTs.

DISCUSSION

RATIONALE FOR THE *LOGIT* FUNCTION

Underlying every decompression table is a judgment or belief about how DCS is related to the variables that a dive entails — depth, bottom time, TDT, and any others. With probabilistic modeling, this belief is embodied in the equation or algorithm used to fit the calibration data. From collective experience, we presume that — except for dive depth and bottom time — TDT is by far the most important determinant of DCS risk. In practice, it is desirable to have TDT as short as possible and bottom time as long as possible; depth is determined by the job requirement. Next in importance is probably the particular pattern of depth and time duration at stops. Other important determinants of DCS risk, but in uncertain order, are variables such as the kind of dive (dry or in the water), the intensity of exercise, and the environmental temperature. Previous probabilistic decompression models[1,2,10,19–22] used elements of traditional knowledge about the etiology of DCS:

1) the idea that the body is composed of several "tissue compartments" that exchange inert gas at various rates,

2) the idea that the supersaturation which a particular tissue can tolerate without developing DCS is limited, and

3) the idea, in some models,[19,20] that diffusive exchange of gas bubbles is an important variable.

Recent models use time of DCS onset to attempt to refine risk estimates.[21,22] Some variables — e.g., bubbles detected in venous blood and the times at which symptoms occur — concern the course of the DCS disease process rather than the cause of the process. Use of such variables in fitting equations may actually contribute to bias rather than help to estimate *Pdcs* of particular dives.

The basis for Equation 4 is the obvious statement that for dives with depths and bottom times that put divers outside the region of "no-stop" diving, DCS can be avoided by time spent at decompression stops. In no-stop diving there is a hyperbolic relationship between dive depth and bottom time; this hyperbolic relationship may mean that DCS can result from an excessive "dose" of depth multiplied by time ($D \bullet T$). We carry that notion into our present analysis of decompression-stop dives by considering that time at decompression stops

serves as an "antidote" to a dose of ($D \bullet T$) that would be intolerable for a no-stop dive. Thus, for a given ($D \bullet T$) product, probability of DCS is low if TDT is large.

In our graphical analysis[3] we plotted TDTs versus bottom times for a particular depth, similar to the graphs in Figures 1, 8, 9, and 10, for several decompression tables. Figure 11 shows the traces for many depths generated from the deterministic VVal-18 Algorithm.[4,5] All tables we examined showed the same pattern: a fan of lines seemed to originate at a point on the zero bottom-time axis at a negative TDT.

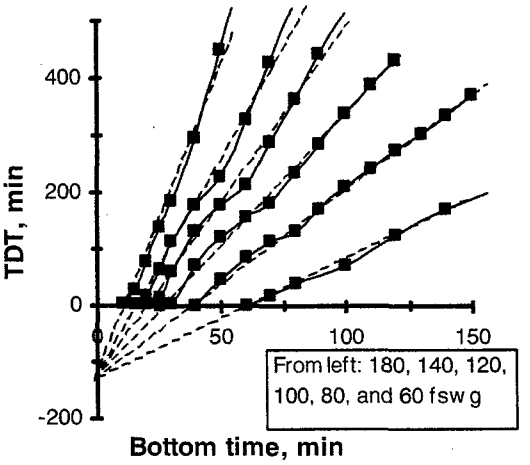

FIGURE 11. Bottom-time/TDT combinations according to the VVal-18 Algorithm for several depths. Dashed projection lines are drawn by eye.

We used the fan idea and a combination of insight with trial and error to devise Equation 4. A simple equation for the reciprocal of the slope of one of the projection lines in Figure 11 is $Y_1 = T/(TDT - g)$, where Y_1 is defined by the equation, T is bottom time, TDT is total decompression time, and g is the intersection of the line with the TDT axis at zero bottom time. The fan shape could be accommodated by adding depth to the formula: $Y_2 = D \bullet T/(TDT - g)$. We found empirically that subtracting a constant from depth improved the fit of the data: $Y_3 = (D - c) \bullet T/(TDT - g)$. To account for the expectation that bottom time levels off as tissues become saturated with inert gas, we changed the bottom-time term: $Y_4 = (D - c) \bullet [1 - \exp(-d \bullet T)]/(TDT - g)$, where d regulates the rate of leveling off. Finally, we raised bottom time to a power to allow the possibility that the leveling off might not correspond to a single exponential function: $Y_5 = (D - c) \bullet [1 - \exp(-d \bullet T^f)]/(TDT - g)$. Assuming that the probability of DCS is related to the Y_5 formulation gives the final function, Equation 4:

$$LOGIT = a + b \cdot (D - c) \cdot \left(\frac{1 - e^{\left(-d \cdot T^f\right)}}{TDT - g} \right) \qquad (4)$$

When we used these various Y_i alternatives in $LOGIT$ functions, each of the changes significantly improved the log-likelihood number according to the likelihood ratio test.

Conventional tables generated by both deterministic[4,5,23–25] and probabilistic[1,2,10,19–21] models account for the inert gas partial pressures in a series of tissue compartments during depth/time maneuvers in a dive profile. A

decompression stop is prescribed whenever a compartment is at risk of developing DCS. Our simple StandAir Model, generated from the *LOGIT* function given by Equation 4, does not track tissue compartments during the dive, so it cannot prescribe decompression stop depths and times and is therefore not appropriate for operational use, although it is appropriate for estimating risk.

DOSE-RESPONSE CURVES

Figures 1, 8, 9, and 10 illustrate how the long TDTs mandated by the NMRI-98 Model[2] are not warranted. Dose-response curves illuminate differences between both the NMRI-98 and NMRI-93[10] Models and our StandAir Model. Figures 12A and 12B show specific complete dose-response curves for the StandAir Model. In Figure 12A, bottom time and TDT are held constant, and depth varies. The curve flattens at its upper and lower extremes, so that for a given change in the X-axis variable, the change of *Pdcs* decreases. For example, when bottom time

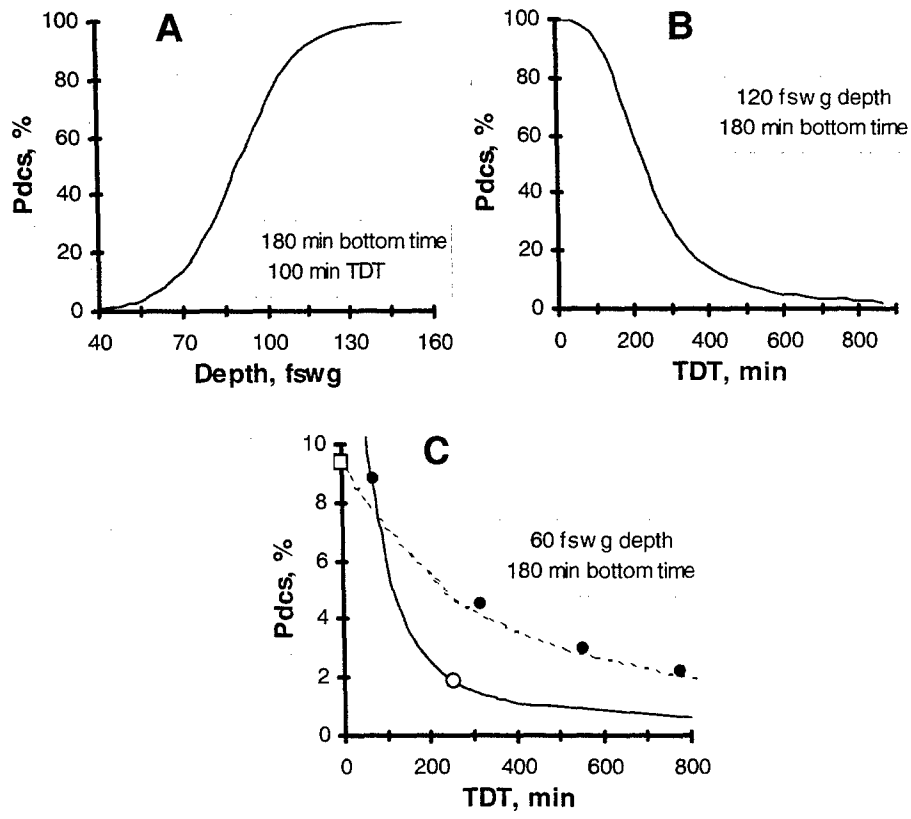

Figure 12. Dose-response relationships. Solid curves = StandAir Model. A: complete dose-response curve when depth is variable. B: complete dose-response curve when TDT is variable. C: low-*Pdcs* range of a dose-response curve for the StandAir Model (solid curve), with information from the NMRI-93 and NMRI-98 Models included; an open circle = TDT value from the VVal-18 Algorithm, with *Pdcs* calculated by the StandAir Model; a dashed curve = NMRI-93 Model; a square = the direct-ascent point for the NMRI-93 Model; filled symbols = selected points from the NMRI-98 Model.

is 180 min and TDT is 100 min, as in Figure 12A, *Pdcs* is 8% for a depth of 64 fswg, and 4% for a depth of 56 fswg — 8 fswg less. Subtracting another 8 fswg reduces *Pdcs* to 2%.

In Figure 12B, depth and bottom time are constant, and TDT varies. Only the low-probability ranges of Figures 12A and 12B are of practical interest for safe diving; DCS rates above 3% are undesirable, except in very unusual circumstances. Whereas increase in depth results in higher probability of DCS in Figure 12A, increase of TDT reduces *Pdcs* in Figure 12B. The practical effect of the leveling of the curve is that smaller increases of TDT are required to improve safety during risky dives than are required to improve safety during relatively safe dives.

The solid curve in Figure 12C shows *Pdcs* plotted as a function of various TDTs for 180-minute dives to 60 fswg. The open circle on the curve illustrates the TDT required by the VVal-18 Algorithm; according to the StandAir Model, the 254 min of TDT gives a DCS risk of less than 2%. The dashed trace is taken from Table 2 in the report concerned with NMRI-93.[10] The dashed trace is less steep than the solid curve at the left and has much less curvature than the solid curve in the middle of the graph, so that it does not reach the low *Pdcs* range until TDT is very high. According to the NMRI-93 Model, a TDT of more than 800 min is required for the same risk shown by the VVal-18 point. Thus, Figure 12C shows that in the range of operational diving, the NMRI-93 Model is much more conservative than the StandAir and VVal-18 Models. The NMRI-98 Model is also conservative: the filled symbols fall close to the NMRI-93 curve.

The two curves in Figure 12C cross where *Pdcs* is about 7.5%. To the left of the crossover, the relative risks predicted by the StandAir and NMRI-93 models are reversed. For TDTs less than 82 min, the NMRI-93 Model is less conservative than the StandAir Model; the NMRI-93 Model requires less TDT time than the StandAir Model for the same risk, or, for a given TDT, estimated *Pdcs* is less than for the StandAir Model. The square at 9.5% *Pdcs* shows the risk of DCS of direct ascent from a dive to 60 fswg for 180 min according to the NMRI-93 Model; the StandAir Model predicts that a direct ascent has a much higher risk than does the NMRI-93 Model; the direct-ascent point is at 29% *Pdcs*, off the scale of the graph.

Relationships between the dose-response curves for the models change as the diving range changes. Figure 13 shows dose-response comparisons for several depth/bottom-time combinations. The three left-hand panels, for dives with short bottom times, show that the crossover point moves toward higher TDT as depth increases. Thus, in Figure 13C the StandAir, NMRI-93, and NMRI-98 Models are all between 2 and 3% *Pdcs* when TDT is between 100 and 150 min. In Figure 13E the NMRI-93 Model actually requires less TDT time than the StandAir Model requires when *Pdcs* is 2%; the NMRI-93 Model is less conservative than the StandAir Model to the left of the crossover.

The three right-hand panels in Figure 13 show that with long bottom times, the StandAir Model requires much shorter TDTs than the NMRI-93 and NMRI-98 Models require. The crossover is at TDT of about 200 min for all the depths shown.

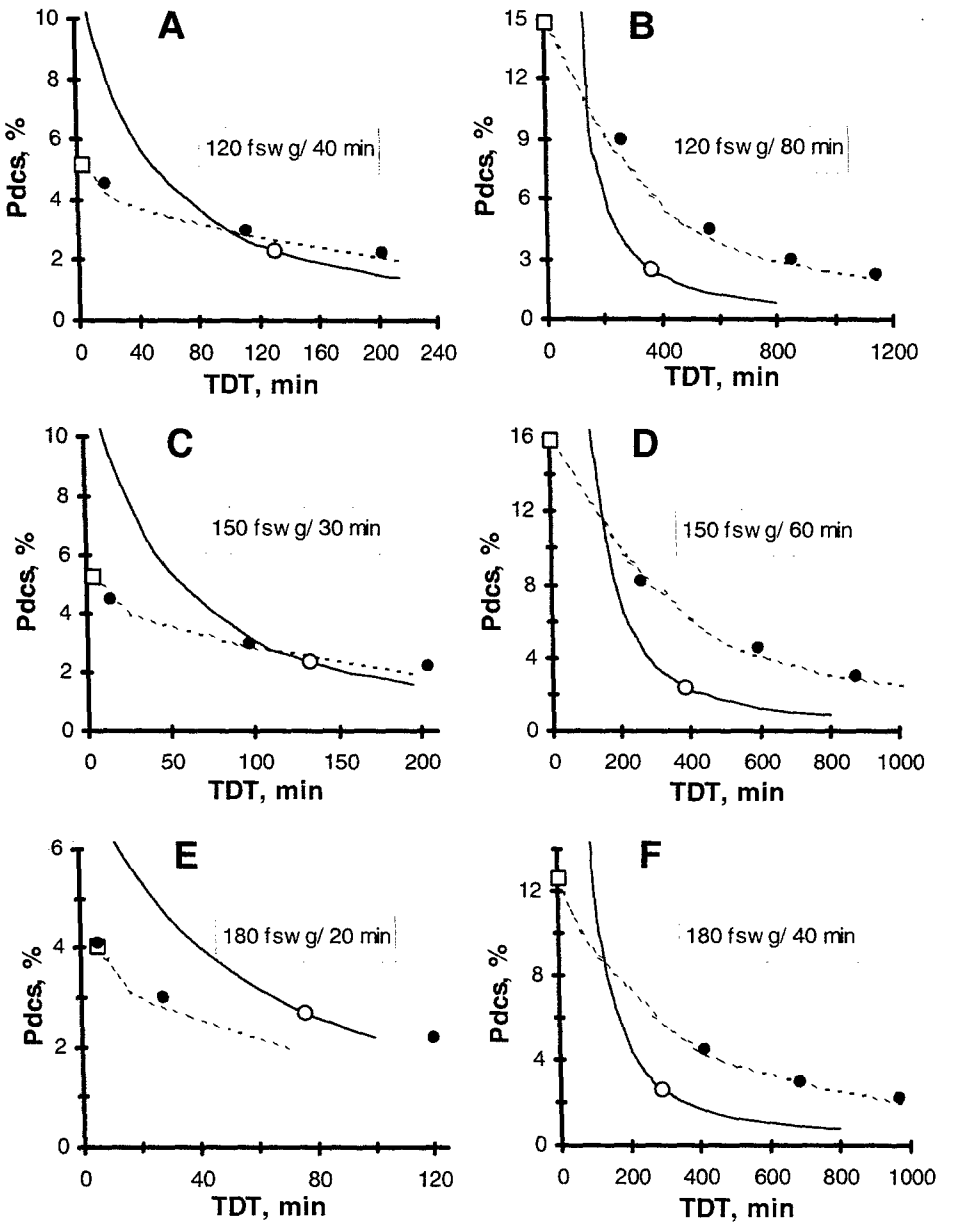

Figure 13. Dose-response curves for a variety of bottom times and depths. Solid curves = StandAir Model, dashed curves = NMRI-93 Model, filled black symbols = selected points from the NMRI-98 Model, open circles = TDT values from the VVal-18 Algorithm with *Pdcs* calculated by the StandAir Model, and squares = direct-ascent points for the NMRI-93 Model.

OPERATIONAL DIVING: VVAL-18 ALGORITHM AND USN57

The framework established by the statistical process is the essential element of a probabilistic model, but the framework may be flawed. The statistical process fits all regions as well as possible, but the fit may be poor in a region of particular interest, such as the operationally important region of low *Pdcs*. Regions that are particularly vulnerable to error are at the edges of the range of the model, where prescriptions tend to be extrapolations from the bulk of the calibration data. To become aware of problem areas, we advocate using observed data retrospectively — as in Figures 9 and 10 — to evaluate model prescriptions in low-*Pdcs* regions.

We find no reason for concern about the StandAir Model's prescriptions for deep dives that have appreciable TDTs: the DCS cases for these are below the 2% table traces in Figure 9, evidence that that the StandAir Model is effective in prescribing TDTs that avoid DCS. It follows that the long TDTs prescribed by NMRI-98 and similar models[2,10] are not warranted, but this conclusion is weakened by a lack of dives, especially DCS-free dives, in the long-TDT region. In the absence of data in a depth/bottom time/TDT region, a model's estimates in that region are extrapolations and interpolations from data-rich regions; thus, the StandAir Model's prescriptions for long TDT tend to be projections from short-TDT regions.

For dives shallower than 60 fswg, the calibration dataset has 641 person-dives with 35 DCS cases, but average TDT for these is only 3.5 min. This means that the StandAir Model's TDT values for depths shallower than 60 fswg are extrapolations from deeper dives that have appreciable TDTs. For shallow dives, especially for 40 fswg, we therefore believe that the StandAir Model prescriptions for TDTs are questionable.

No-stop dives

No-stop time limits for the USN57 Table and the VVal-18 Algorithm are in columns 2 and 3 of Table 3. Times for 2% *Pdcs* according to the StandAir Model are in Column 4. Deeper than 50 fswg, StandAir Model prescriptions for 2% *Pdcs* tend to agree with those of VVal-18; the maximum difference between the two models is 3 minutes for depths between 70 to 120 fswg. No-stop bottom times for the StandAir Model are less conservative (i.e., they allow longer bottom times at a given depth) than USN57 for depths shallower than 35 fswg and deeper than 80 fswg. The difference is as large as 10 min at 150 fswg.

Evaluation graphs for depths shallower than 40 fswg are not feasible because the calibration dataset lacks shallow person-dives. The evaluation graph for 40 fswg in Figure 10 has few person-dives and the table traces are widely separated, but the 2% *Pdcs* trace for the StandAir Model lies to the left of the triangle and thus avoids the DCS case. For dives shallower than 50 fswg in

TABLE 3. NO-STOP BOTTOM-TIME LIMITS FROM THREE SOURCES

(1) Depth, fswg	(2) USN57	(3) VVal18 Algorithm	(4) ← StandAir model 2%	(5) 1%	(6) → 3%
25	**595**	1,103	*	*	*
30	**405**	372	**1,188**	485	*
35	**310**	232	**301**	175	395
40	**200**	163	**173**	105	219
50	**100**	92	**92**	57	114
60	**60**	63	**62**	39	76
70	**50**	49	**46**	30	57
80	**40**	40	**37**	24	45
90	**30**	34	**31**	20	38
100	**25**	29	**26**	17	32
110	**20**	26	**23**	15	28
120	**15**	23	**20**	13	25
130	**10**	19	**18**	12	22
140	**10**	17	**16**	11	20
150	**5**	14	**15**	10	18
160	**5**	12	**14**	9	17
170	**5**	11	**13**	8	16
180	**5**	10	**12**	8	15
190	**5**	9	**11**	7	14

* = more than 1,440 min

Table 3, the StandAir prescriptions are more liberal than those of the VVal-18 Algorithm. For no-stop dives shallower than 50 fswg, it seems reasonable to recommend bottom times longer than those for the VVal-18 Algorithm but not as long as those for USN57.

The deepest dives raise a question about the StandAir Model's prescriptions for no-stop dives. In Figure 10 there is a gray triangle for profiles having short TDT at 170 fswg (the dive is 165 fswg for 10 min bottom time and 18 min TDT), a nearby white triangle at 170 fswg (168 fswg, for 10 min bottom time and 18 min TDT), and a white triangle near the no-stop point at 150 fswg (146 fswg, 15.5 min bottom time, and 2.5 min TDT). In addition, there are three DCS cases for deeper depths (one case at 198 fswg, 9 min bottom time, and 3.3 min TDT; and two cases at 231 fswg, 6.8 min bottom time, and 3.9 min TDT).

This pattern of DCS cases for short, deep dives is reason to believe that the no-stop bottom times for both the VVal-18 Algorithm and the StandAir Model are too long. For dives deeper than 130 fswg, we recommend bottom times two or three minutes shorter than those shown for the VVal-18 Algorithm in column 3 of Table 3 — bottom times near those shown for 1% *Pdcs* by the StandAir Model, but not as short as those for USN57. Thus, for 180 and 190 fswg we recommend bottom times closer to the 5 min allowed by the U.S. Navy Standard Air Table than to the 11- or 12-minute prescriptions of our StandAir Model.

Pdcs for the VVAL-18 Algorithm, the NMRI-98 Model, and USN57

Our simple StandAir Model cannot prescribe decompression stop depths and times and is therefore not appropriate for operational use. However, the general concurrence between prescriptions of our model and those of the deterministic VVal-18 Algorithm[4,5] indicate that the VVal-18 Algorithm is acceptable for operational use for most depths. Deterministic models do not yield estimates of *Pdcs* for various dive profiles, but assuming that our StandAir Model gives valid *Pdcs* estimates, we can generate probability values for the depth/bottom-time/TDT profiles prescribed by the VVal-18 Algorithm.

Table A1 of the Appendix allows comparison of our StandAir Model and the VVal-18 Algorithm. Discontinuities in the table result from different bottom times used by the two models for no-stop dives and for a few dives with short TDT. Column 1 of Table A1 marks the no-stop prescriptions for the StandAir Model (S) and the VVal-18 Algorithm (V), and columns 2 and 3 give depths and bottom times. Column 4 gives the TDT associated with 2% *Pdcs* according to the StandAir Model, and low and high confidence intervals (CI) around 2% *Pdcs* are in columns 5 and 6. Column 7 gives TDT for the VVal-18 Algorithm, and column 8 gives the *Pdcs* estimate based on StandAir Model parameters for the depth/bottom-time/TDT combinations of the table generated from the VVal-18. The TDT values of the two models in Table A1 are similar for most depths, in accord with the closeness of VVal-18 traces to the 2% traces for the StandAir Model in Figures 8A, 9, and 10. Column 9 gives the TDT ratio (TDT for StandAir divided by TDT for VVal-18). The TDT for the StandAir Model is both above and below that for VVal-18, but the ratio is sometimes well above 1.0 for short-TDT dives deeper than 90 fswg. The average ratio is 1.30 ± 0.79 SD, with a range from 0.55 to 7.04.

Table A2 of the Appendix gives estimates of CIs for the VVal-18 Algorithm; the *Pdcs* column repeats information from Table A1. The *Pdcs* average is 2.28 ± 0.34% (SD), close to 2%. According to the trend curve in Figure 7B, *Pdcs* of 2.28% is associated with observed incidence of 1.65%.

Figure 14A shows *Pdcs* and 95% CIs estimated by our StandAir Model for individual profiles of a table generated from the VVal-18 Algorithm.[4,5] Points are for individual profiles listed as they appear in Table A1 — that is, according to depth, and within depth according to bottom times. For example, the leftmost point is for a 40 fswg dive for 163 minutes, the second-to-left point is for 40 fswg for 200 minutes, and the farthest right point is for 190 fswg for 40 min. Figure 14B shows *Pdcs* and 95% CIs for individual profiles of the VVal-18 table as estimated by the NMRI-93 Model;[10] the plotted values are taken from Thalmann's publication.[4] The *Pdcs* values are much higher than those in Table A2, and the greatest differences between *Pdcs* estimates by the NMRI-93 and StandAir Models occur at the longest bottom times for a particular depth.

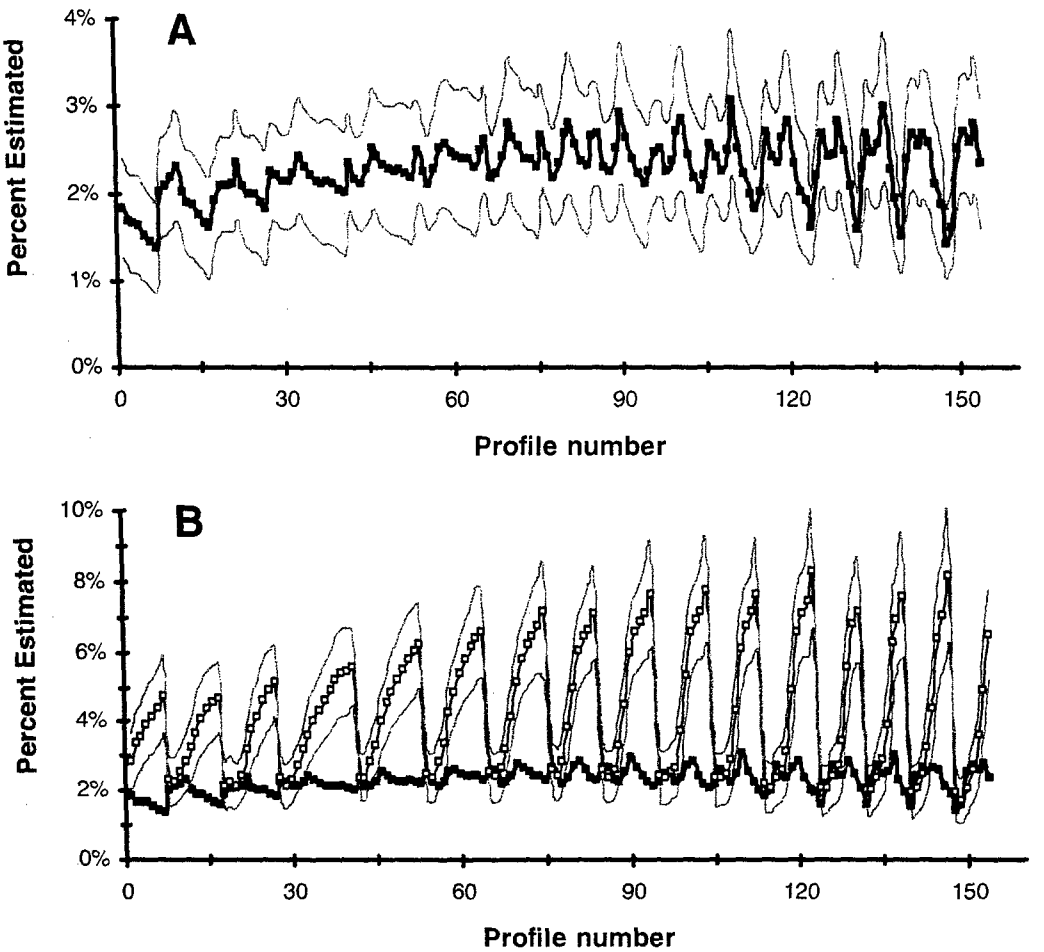

Figure 14. Probability of DCS and 95% confidence intervals for profiles of a table generated from the VVal-18 Algorithm; estimates are calculated by two probabilistic models. A: *Pdcs* and 95% confidence intervals estimated by the StandAir Model. B: as in Panel A, but estimated by the NMRI-93 Model; the StandAir *Pdcs* trace is repeated from Panel A.

Figure 15 shows *Pdcs* estimated by our StandAir Model for a NMRI-98 table. The NMRI-98 table was generated to have *Pdcs* of 2.2%, but the StandAir estimates show *Pdcs* as low as 0.33% (profile #17, for 40 fswg for 720 min). Profiles #150 to #158 are for the dives to 150 fswg that were illustrated in Figures 1 and 8; because the NMRI-98 Model mandates long TDTs for dives with long bottom times, estimated *Pdcs* is low.

As we noted in discussing Figure 1, USN57 appears to prescribe too little time at decompression stops. Columns 4, 5, and 6 in Appendix Table A3 list probability estimates with 95% CIs calculated by our StandAir Model for the USN57 table. Table A3 also gives two additional probability estimates with 95% CIs for the USN57 table: by the NMRI-98 Model[2] (columns 7–9; personal communication; K. Gault, 1998), and by the NMRI-93 Model[10] (columns 10–12, from Thalmann[4]).

The *Pdcs* and CIs estimated by all three models are high and variable: average *Pdcs* = 8.3 ± 5.7% (SD) and the range is from 0.6 to 21.4% for the StandAir Model; average *Pdcs* = 8.1 ± 5.0% (SD) for the NMRI-98 Model and 6.3 ± 4.0% (SD) for the NMRI-93 Model.

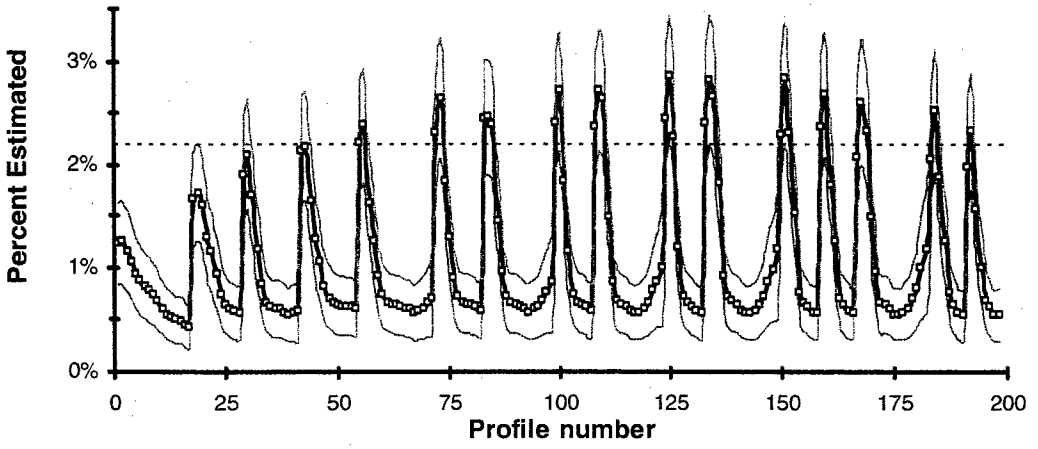

Figure 15. Probability of DCS estimated by our StandAir Model, with 95% confidence intervals, for the NMRI-98 table generated to have putative *Pdcs* of 2.2% (horizontal dashed line). The highest points on the saw tooth pattern are for no-stop dives, and the low points are for dives with long TDTs.

CONCLUSIONS

1. Our probabilistic StandAir Model, generated from nonsaturation dives only, appears to prescribe TDT times that are acceptable for standard air diving to most depths. Questionable model prescriptions are at the two extremes of the depth continuum: few dives have appreciable time at decompression stops at the shallowest depths, and cases of DCS near the StandAir Model prescriptions for dives with short TDTs suggest that the model may be too liberal for deep no-stop dives and for deep dives having short TDTs.
2. According to our StandAir Model, the long times at decompression stops mandated by some other probabilistic models are not warranted. The failure of these other models to provide reasonable prescriptions for standard air dives means that their estimates of *Pdcs* for standard air dives are also inaccurate.
3. Estimates using the StandAir Model parameters indicate that the VVal-18 algorithm gives *Pdcs* near 2% and therefore is acceptable for operational use to most depths.

REFERENCES

1. P. K. Weathersby, L. D. Homer, and E. T. Flynn, "On the Likelihood of Decompression Sickness," *J Appl Physiol*, Vol. 57 (1984), pp. 815–824.

2. E. C. Parker, S. S. Survanshi, P. B. Massell, and P. K. Weathersby, "Probabilistic Models of the Role of Oxygen in Human Decompression Sickness," *J Appl Physiol*, Vol. 84 (March 1998), pp. 1096–1102.

3. H. D. Van Liew and E. T. Flynn, *Graphical Analysis: Decompression Tables and Dive-Outcome Data*, NEDU TR 04-40, Navy Experimental Diving Unit, Dec 2004.

4. E. D. Thalmann, *Suitability of the USN MK 15 (VVAL-18) Decompression Algorithm for Air Diving*, NEDU TR 03-12, Navy Experimental Diving Unit, Aug 2003 (originally published as Final Report on Research Contract N0463A-96-M-7036, March 30, 1997).

5. E. D. Thalmann, *Phase II Testing of Decompression Algorithms for Use in the U.S. Navy Underwater Decompression Computer*, NEDU TR 1-84, Navy Experimental Diving Unit, Jan 1984.

6. Commander, Naval Sea Systems Command, *U.S. Navy Diving Manual, Revision 4*, SS521-AG-PRO-010 (Arlington, VA: NAVSEA, 1999).

7. P. K. Weathersby, S. S. Survanshi, L. D. Homer, B. L. Hart, R. Y. Nishi, E. T. Flynn, and M. E. Bradley, *Statistically Based Decompression Tables. I Analysis of Standard Air Dives: 1950–1970*, Naval Medical Research Institute (NMRI) Technical Report 85-16, Bethesda, MD, 1985.

8. F. K. Butler and D. Southerland, "The U.S. Navy Decompression Computer," *Undersea Hyper Med*, Vol. 28 (Fall 2001), pp. 213–228.

9. H. D. Van Liew and E. T. Flynn, "Probabilistic Models for Standard Air Dives: Effect of Inclusion of Saturation Data," *Undersea Hyperbaric Med*, Vol. 28 (Supplement 2001), p. 41.

10. S. S. Survanshi, E. D. Parker, E. D. Thalmann, and P. K. Weathersby, *Statistically Based Decompression Tables XII, Volume I: Repetitive Decompression Tables for Air and Constant 0.7 ATA PO_2 in N_2 Using a Probabilistic Model*, Naval Medical Research Institute (NMRI) Technical Report 97-36, Bethesda, MD, 1997.

11. D. J. Temple, R. Ball, P. K. Weathersby, E. C. Parker, and S. S. Survanshi, *The Dive Profiles and Manifestations of Decompression Sickness Cases after*

Air and Nitrogen-Oxygen Dives, Volumes I and II, Naval Medical Research Center (NMRC) Technical Report 99-02, Bethesda, MD, 1999.

12. P. K. Weathersby, S. S. Survanshi, R. Y. Nishi, and E. D. Thalmann, *Statistically Based Decompression Tables VII: Selection and Treatment of Primary Air and N_2O_2 Data*, Joint Report, U.S. Naval Submarine Medical Research Laboratory, rep. 1182, Groton, CT; Naval Medical Research Institute (NMRI) Technical Report 92-85, Bethesda, MD, 1992.

13. E. D. Thalmann, E. C. Parker, S. S. Survanshi, and P. K. Weathersby, "Improved Probabilistic Decompression Model Risk Predictions Using Linear-Exponential Kinetics," *Undersea Hyper Med*, Vol. 24 (Winter 1997), pp. 255–274.

14. G. J. Duffner and H. H. Snider, *Effects of Exposing Men to Compressed Air and Helium-Oxygen Mixtures for 12 Hours at Pressures of 2–2.6 Atmospheres*, NEDU TR 1-59, Navy Experimental Diving Unit, 1959.

15. L. Wilkinson, *SYSTAT: The System for Statistics* (Evanston, IL: SYSTAT, Inc., 1990).

16. H. H. Ku, "Notes on the Use of Propagation of Error Formulas," *Journal of Research of the National Bureau of Standards. C, Engineering and Instrumentation*, Vol. 70C (October-December 1966), pp. 263–273.

17. H. D. Van Liew and E. T. Flynn, "Use of Dive-Outcome Information Three Times in Preparation of a Probabilistic Decompression Model," *Undersea Hyperbaric Med*, Vol. 29 (Summer 2002), pp. 111–112.

18. H. D. Van Liew and E. T. Flynn, *Probability of Decompression Sickness in No-Stop Air Diving*, NEDU TR 04-42, Navy Experimental Diving Unit, Dec 2004.

19. W. A. Gerth and R. D. Vann, "Probabilistic Gas and Bubble Dynamics Models of Decompression Sickness Occurrence in Air and Nitrogen-Oxygen Diving," *Undersea Hyper Med*, Vol. 24 (Winter 1977), pp. 275–292.

20. P. Tikuisis, K. A. Gault, and R. Y. Nishi, "Prediction of Decompression Illness Using Bubble Models," *Undersea Hyperbaric Med*, Vol. 21 (June 1994), pp. 129–143.

21. P. K. Weathersby, S. S. Survanshi, L. D. Homer, E. Parker, and E. D. Thalmann, "Predicting the Time of Occurrence of Decompression Sickness," *J Appl Physiol*, Vol. 72 (1992), pp. 1541–1548.

22. J. Conkin, V. Kumar, M. P. Powell, P. P. Foster, and J. M. Waligora, "A Probabilistic Model of Hypobaric Decompression Sickness Based on 66 Chamber Tests," *Aviat Space Environ Med*, Vol. 67 (February 1996), pp. 176–183.

23. M. L. Gernhardt, "Development and Evaluation of a Decompression Stress Index Based on Tissue Bubble Dynamics" (Ph.D. dissertation, University of Pennsylvania, 1991).

24. C. J. Lambertsen, IFEM / Sub Sea International Inc., *Air Diving Tables*. Institute for Environmental Medicine, University of Pennsylvania, Document NO-S-MA-DTA01, Revision A, Philadelphia PA, 1995.

25. R. Y. Nishi, B. A. Hobson, and G. R. Lauckner, *DCIEM / Canadian Forces Air Decompression Tables and Procedures* (Downsview, Ont., Canada: DCIEM, 1986).

APPENDIX – PROBABILITY ESTIMATES FOR DECOMPRESSION MODELS

TABLE A1. DECOMPRESSION TABLE BASED ON THE STANDAIR MODEL AND COMPARISON WITH THE VVAL-18 ALGORITHM

In column 1, V = VVal-18 Algorithm no-stop; S = StandAir Model no-stop

(1)	(2)	(3)	(4)	(5)	(6)	(7)	(8)	(9)
No-Stop	Depth, fswg	Bottom time, min	TDT, StandAir, min for 2% *Pdcs*	Low CI, *Pdcs*	High CI, *Pdcs*	TDT, VVal-18, min	*Pdcs*, VVal-18	TDT ratio, SA / VVal
V	40	163	---	---	---	**0.7**	1.8%	---
S	40	173	**1.3**	1.4%	2.6%	---	---	---
	40	190	**14**	1.4%	2.6%	---	---	---
	40	200	**21**	1.4%	2.6%	**39**	1.7%	0.55
	40	210	**28**	1.3%	2.7%	**48**	1.7%	0.60
	40	230	**42**	1.3%	2.7%	**65**	1.6%	0.66
	40	250	**56**	1.3%	2.7%	**90**	1.5%	0.62
	40	270	**68**	1.3%	2.7%	**113**	1.4%	0.61
	40	300	**87**	1.3%	2.7%	**142**	1.4%	0.61
V	50	92	---	---	---	**0.8**	2.0%	---
S	50	92	**1.7**	1.5%	2.5%	---	---	---
	50	100	**14**	1.4%	2.6%	**10**	2.1%	1.44
	50	110	**29**	1.4%	2.6%	**21**	2.2%	1.41
	50	120	**44**	1.4%	2.6%	**30**	2.3%	1.47
	50	140	**72**	1.4%	2.6%	**71**	2.0%	1.02
	50	160	**99**	1.4%	2.6%	**106**	1.9%	0.94
	50	180	**125**	1.4%	2.6%	**135**	1.9%	0.93
	50	200	**150**	1.3%	2.7%	**171**	1.8%	0.88
	50	220	**174**	1.3%	2.7%	**208**	1.7%	0.84
	50	240	**196**	1.3%	2.7%	**239**	1.6%	0.82
S	60	62	**2.0**	1.5%	2.5%	---	---	---
V	60	63	---	---	---	**1.0**	2.1%	---
	60	70	**21**	1.5%	2.5%	**17**	2.1%	1.25
	60	80	**44**	1.5%	2.5%	**38**	2.1%	1.16
	60	100	**88**	1.4%	2.6%	**70**	2.3%	1.26
	60	120	**130**	1.4%	2.6%	**124**	2.1%	1.05
	60	140	**170**	1.4%	2.6%	**170**	2.0%	1.00
	60	160	**208**	1.3%	2.7%	**208**	2.0%	1.00
	60	180	**244**	1.3%	2.7%	**254**	1.9%	0.96
	60	200	**279**	1.3%	2.7%	**297**	1.8%	0.94
S	70	46	**2.3**	1.5%	2.5%	---	---	---
V	70	49	---	---	---	**1.2**	2.2%	---
	70	50	**14**	1.5%	2.5%	**5**	2.2%	2.71
	70	60	**46**	1.5%	2.5%	**39**	2.1%	1.16
	70	70	**76**	1.5%	2.5%	**68**	2.1%	1.12
	70	80	**106**	1.4%	2.6%	**92**	2.2%	1.15

	70	90	**134**	1.4%	2.6%	**108**	2.4%	1.24
	70	100	**162**	1.4%	2.6%	**141**	2.3%	1.15
	70	110	**190**	1.4%	2.6%	**173**	2.2%	1.10
	70	120	**216**	1.4%	2.6%	**203**	2.2%	1.06
	70	130	**242**	1.3%	2.7%	**230**	2.1%	1.05
	70	140	**267**	1.3%	2.7%	**253**	2.1%	1.06
	70	150	**292**	1.3%	2.7%	**280**	2.1%	1.04
	70	160	**316**	1.3%	2.7%	**310**	2.1%	1.02
70	170	340	**1.3%**	2.7%	338	**2.0%**	1.00	
S	80	37	**2.7**	1.5%	2.5%	**---**	---	---
V	80	40	**6**	1.4%	2.6%	**1.3**	2.4%	4.42
	80	50	**55**	1.5%	2.5%	**47**	2.2%	1.16
	80	60	**94**	1.5%	2.5%	**86**	2.1%	1.09
	80	70	**131**	1.4%	2.6%	**113**	2.3%	1.16
	80	80	**167**	1.4%	2.6%	**133**	2.5%	1.25
	80	90	**202**	1.4%	2.6%	**170**	2.4%	1.19
	80	100	**236**	1.4%	2.6%	**209**	2.3%	1.13
	80	110	**270**	1.3%	2.7%	**244**	2.3%	1.10
	80	120	**302**	1.3%	2.7%	**275**	2.3%	1.10
	80	130	**334**	1.3%	2.7%	**304**	2.3%	1.10
	80	140	**365**	1.3%	2.7%	**336**	2.2%	1.08
	80	150	**395**	1.3%	2.7%	**370**	2.2%	1.07
S	90	31	**3.0**	1.5%	2.5%	**---**	---	---
V	90	34	**---**	---	---	**1.5**	2.5%	---
	90	40	**49**	1.5%	2.5%	**37**	2.3%	1.34
	90	50	**96**	1.5%	2.5%	**89**	2.1%	1.09
	90	60	**142**	1.4%	2.6%	**124**	2.3%	1.15
	90	70	**186**	1.4%	2.6%	**151**	2.5%	1.24
	90	80	**229**	1.4%	2.6%	**186**	2.6%	1.23
	90	90	**270**	1.4%	2.6%	**229**	2.5%	1.18
	90	100	**311**	1.3%	2.7%	**271**	2.4%	1.15
	90	110	**350**	1.3%	2.7%	**308**	2.4%	1.14
	90	120	**388**	1.3%	2.7%	**344**	2.4%	1.13
	90	130	**426**	1.3%	2.7%	**387**	2.3%	1.10
S	100	26	**3.3**	1.5%	2.5%	**---**	---	---
V	100	29	**---**	---	---	**1.7**	2.5%	---
	100	30	**26**	1.5%	2.5%	**4**	2.6%	7.04
	100	40	**83**	1.5%	2.5%	**73**	2.2%	1.14
	100	50	**137**	1.5%	2.5%	**122**	2.2%	1.13
	100	60	**190**	1.4%	2.6%	**159**	2.4%	1.20
	100	70	**241**	1.4%	2.6%	**184**	2.8%	1.31
	100	80	**290**	1.4%	2.6%	**236**	2.6%	1.23
	100	90	**338**	1.3%	2.7%	**285**	2.6%	1.19
	100	100	**385**	1.3%	2.7%	**340**	2.4%	1.13
	100	110	**430**	1.3%	2.7%	**388**	2.3%	1.11
	100	120	**474**	1.3%	2.7%	**434**	2.3%	1.09
S	110	23	**3.7**	1.5%	2.5%	**---**	---	---
	110	25	**19**	1.5%	2.5%	**---**	---	---
V	110	26	**---**	---	---	**1.8**	2.7%	---
	110	30	**52**	1.5%	2.5%	**33**	2.4%	1.58
	110	40	**116**	1.5%	2.5%	**105**	2.2%	1.11

	110	50	**178**	1.4%	2.6%	**153**	2.4%	1.17
	110	60	**238**	1.4%	2.6%	**187**	2.7%	1.27
	110	70	**296**	1.4%	2.6%	**230**	2.8%	1.29
	110	80	**352**	1.3%	2.7%	**295**	2.6%	1.19
	110	90	**406**	1.3%	2.7%	**362**	2.4%	1.12
	110	100	**459**	1.3%	2.7%	**416**	2.3%	1.10
S	120	20	**4.0**	1.5%	2.5%	**---**	---	---
V	120	23	**---**	---	---	**2.0**	2.7%	---
	120	25	**41**	1.5%	2.5%	**15**	2.7%	2.73
	120	30	**78**	1.5%	2.5%	**62**	2.3%	1.26
	120	40	**150**	1.5%	2.5%	**132**	2.3%	1.14
	120	50	**219**	1.4%	2.6%	**180**	2.5%	1.22
	120	60	**286**	1.4%	2.6%	**215**	2.9%	1.33
	120	70	**350**	1.3%	2.7%	**289**	2.6%	1.21
	120	80	**413**	1.3%	2.7%	**365**	2.4%	1.13
	120	90	**474**	1.3%	2.7%	**442**	2.2%	1.07
	120	100	**533**	1.3%	2.7%	**515**	2.1%	1.03
S	130	18	**4.3**	1.5%	2.5%	**---**	---	---
V	130	19	**---**	---	---	**2.2**	2.3%	---
	130	20	**21**	1.5%	2.5%	**3**	2.5%	6.60
	130	25	**63**	1.5%	2.5%	**40**	2.5%	1.58
	130	30	**104**	1.5%	2.5%	**89**	2.3%	1.17
	130	40	**184**	1.4%	2.6%	**157**	2.4%	1.17
	130	50	**260**	1.4%	2.6%	**205**	2.7%	1.27
	130	60	**334**	1.4%	2.6%	**260**	2.9%	1.28
	130	70	**405**	1.3%	2.7%	**355**	2.4%	1.14
	130	80	**475**	1.3%	2.7%	**448**	2.2%	1.06
	130	90	**542**	1.3%	2.7%	**533**	2.1%	1.02
S	140	16	**4.7**	1.5%	2.5%	**---**	---	---
V	140	17	**---**	---	---	**2.3**	2.2%	---
	140	20	**39**	1.5%	2.5%	**16**	2.6%	2.40
	140	25	**86**	1.5%	2.5%	**63**	2.4%	1.35
	140	30	**131**	1.5%	2.5%	**113**	2.3%	1.15
	140	40	**218**	1.4%	2.6%	**180**	2.5%	1.21
	140	50	**301**	1.4%	2.6%	**227**	2.9%	1.33
	140	60	**382**	1.3%	2.7%	**327**	2.5%	1.17
	140	70	**460**	1.3%	2.7%	**428**	2.2%	1.07
	140	80	**536**	1.3%	2.7%	**534**	2.0%	1.00
V	150	14	**---**	---	---	**2.5**	1.8%	---
	150	15	**---**	---	---	**5**	2.0%	---
S	150	15	**5.0**	1.5%	2.5%	**---**	---	---
	150	20	**57**	1.5%	2.5%	**29**	2.7%	2.01
	150	25	**108**	1.5%	2.5%	**85**	2.4%	1.28
	150	30	**157**	1.4%	2.6%	**134**	2.3%	1.17
	150	40	**251**	1.4%	2.6%	**202**	2.6%	1.25
	150	50	**342**	1.4%	2.6%	**270**	2.8%	1.27
	150	60	**430**	1.3%	2.7%	**387**	2.4%	1.11
	150	70	**515**	1.3%	2.7%	**513**	2.0%	1.01
	150	80	**597**	1.3%	2.7%	**613**	1.9%	0.98
V	160	12	**---**	---	---	**2.7**	1.6%	---
S	160	14	**5.3**	1.3%	2.7%	**---**	---	---

	160	15	**20**	1.4%	2.6%	**11**	2.2%	1.83
	160	20	**76**	1.5%	2.5%	**45**	2.7%	1.69
	160	25	**130**	1.5%	2.5%	**105**	2.4%	1.24
	160	30	**183**	1.4%	2.6%	**152**	2.5%	1.21
	160	40	**285**	1.4%	2.6%	**220**	2.8%	1.30
	160	50	**384**	1.3%	2.7%	**331**	2.5%	1.16
	160	60	**478**	1.3%	2.7%	**464**	2.1%	1.03
V	170	11	**---**	---	---	**2.8**	1.6%	---
S	170	13	**5.7**	1.5%	2.5%	**---**	---	---
	170	15	**34**	1.5%	2.5%	**21**	2.3%	1.61
	170	20	**94**	1.5%	2.5%	**61**	2.7%	1.54
	170	25	**152**	1.4%	2.6%	**122**	2.5%	1.25
	170	30	**209**	1.4%	2.6%	**169**	2.6%	1.24
	170	40	**319**	1.4%	2.6%	**240**	3.0%	1.33
	170	50	**425**	1.3%	2.7%	**388**	2.3%	1.09
	170	60	**526**	1.3%	2.7%	**536**	1.9%	0.98
V	180	10	**---**	---	---	**3.0**	1.5%	---
S	180	12	**6.0**	1.5%	2.5%	**---**	---	---
	180	15	**48**	1.5%	2.5%	**30**	2.4%	1.58
	180	20	**112**	1.5%	2.5%	**77**	2.7%	1.46
	180	25	**175**	1.4%	2.6%	**139**	2.5%	1.26
	180	30	**235**	1.4%	2.6%	**185**	2.7%	1.27
	180	40	**353**	1.4%	2.6%	**295**	2.6%	1.20
	180	50	**466**	1.3%	2.7%	**449**	2.1%	1.04
	180	60	**574**	1.3%	2.7%	**598**	1.9%	0.96
V	190	9	**---**	---	---	**3.2**	1.4%	---
	190	10	**---**	---	---	**8**	1.6%	---
S	190	11	**6.3**	1.5%	2.5%	**---**	---	---
	190	15	**62**	1.5%	2.5%	**38**	2.5%	1.62
	190	20	**130**	1.4%	2.6%	**92**	2.7%	1.41
	190	25	**197**	1.4%	2.6%	**156**	2.6%	1.26
	190	30	**262**	1.4%	2.6%	**201**	2.8%	1.30
	190	40	**387**	1.3%	2.7%	**346**	2.4%	1.12

TABLE A2. THE VVAL-18 ALGORITHM: DCS PROBABILITY FOR AIR DIVES ESTIMATED BY THE STANDAIR MODEL

Depth, fswg	Bottom time, min	TDT, min	*Pdcs*, %	Low conf int, %	High conf int, %
40	163	0.7	1.8%	1.3%	2.4%
40	200	38.7	1.7%	1.1%	2.2%
40	210	47.7	1.7%	1.1%	2.2%
40	230	64.7	1.6%	1.1%	2.2%
40	250	89.7	1.5%	1.0%	2.1%
40	270	112.7	1.4%	0.9%	2.0%
40	300	141.7	1.4%	0.9%	1.9%
50	92	0.8	2.0%	1.5%	2.6%
50	100	9.8	2.1%	1.5%	2.7%
50	110	20.8	2.2%	1.6%	2.8%
50	120	29.8	2.3%	1.7%	3.0%
50	140	70.8	2.0%	1.4%	2.6%
50	160	105.8	1.9%	1.3%	2.5%
50	180	134.8	1.9%	1.3%	2.5%
50	200	170.8	1.8%	1.2%	2.4%
50	220	207.8	1.7%	1.1%	2.2%
50	240	238.8	1.6%	1.0%	2.2%
60	60	1.0	1.9%	1.4%	2.4%
60	63	1.0	2.1%	1.6%	2.6%
60	70	17.0	2.1%	1.6%	2.6%
60	80	38.0	2.1%	1.6%	2.7%
60	100	70.0	2.3%	1.7%	3.0%
60	120	124.0	2.1%	1.5%	2.7%
60	140	170.0	2.0%	1.4%	2.6%
60	160	208.0	2.0%	1.3%	2.7%
60	180	254.0	1.9%	1.2%	2.6%
60	200	297.0	1.8%	1.2%	2.5%
70	49	1.2	2.3%	1.7%	2.8%
70	50	5.2	2.2%	1.7%	2.8%
70	60	39.2	2.1%	1.6%	2.7%
70	70	68.2	2.1%	1.6%	2.7%
70	80	92.2	2.2%	1.6%	2.8%
70	90	108.2	2.4%	1.8%	3.1%
70	100	141.2	2.3%	1.6%	3.0%
70	110	173.2	2.2%	1.5%	2.9%
70	120	203.2	2.2%	1.5%	2.8%
70	130	230.2	2.1%	1.4%	2.8%
70	140	253.2	2.1%	1.4%	2.9%
70	150	280.2	2.1%	1.4%	2.8%
70	160	310.2	2.1%	1.3%	2.8%
70	170	338.2	2.0%	1.3%	2.7%
80	40	1.3	2.4%	1.8%	2.9%
80	50	47.3	2.2%	1.6%	2.7%
80	60	86.3	2.1%	1.6%	2.7%
80	70	113.3	2.3%	1.7%	2.9%
80	80	133.3	2.5%	1.8%	3.2%
80	90	170.3	2.4%	1.7%	3.1%
80	100	209.3	2.3%	1.6%	3.0%
80	110	244.3	2.3%	1.6%	3.0%
80	120	275.3	2.3%	1.5%	3.0%
80	130	304.3	2.3%	1.5%	3.0%
80	140	336.3	2.2%	1.5%	3.0%
80	150	370.3	2.2%	1.4%	3.0%
90	34	1.5	2.5%	1.9%	3.1%
90	40	36.5	2.3%	1.7%	2.8%
90	50	88.5	2.1%	1.6%	2.7%
90	60	123.5	2.3%	1.7%	2.9%
90	70	150.5	2.5%	1.8%	3.2%
90	80	185.5	2.6%	1.8%	3.3%
90	90	228.5	2.5%	1.7%	3.2%
90	100	270.5	2.4%	1.7%	3.2%
90	110	307.5	2.4%	1.6%	3.2%
90	120	343.5	2.4%	1.6%	3.2%
90	130	386.5	2.3%	1.5%	3.1%
100	29	1.7	2.5%	1.9%	3.1%
100	30	3.7	2.6%	2.0%	3.2%
100	40	72.7	2.2%	1.7%	2.7%
100	50	121.7	2.2%	1.7%	2.8%
100	60	158.7	2.4%	1.8%	3.1%
100	70	183.7	2.8%	2.0%	3.6%
100	80	235.7	2.6%	1.9%	3.4%
100	90	284.7	2.6%	1.8%	3.4%
100	100	339.7	2.4%	1.6%	3.2%
100	110	381.7	2.4%	1.6%	3.2%
100	120	433.7	2.3%	1.5%	3.1%
110	26	1.8	2.7%	2.1%	3.3%
110	30	32.8	2.4%	1.9%	3.0%
110	40	104.8	2.2%	1.6%	2.7%
110	50	152.8	2.4%	1.7%	3.0%
110	60	186.8	2.7%	2.0%	3.4%
110	70	229.8	2.8%	2.0%	3.6%
110	80	294.8	2.6%	1.8%	3.4%

APPENDIX – PROBABILITY ESTIMATES FOR DECOMPRESSION MODELS

Depth, fswg	Bottom time, min	TDT, min	***Pdcs*, %**	Low conf int, %	High conf int, %
110	90	361.8	2.4%	1.6%	3.2%
110	100	415.8	2.3%	1.5%	3.1%
120	23	2.0	2.7%	2.1%	3.3%
120	25	15.0	2.7%	2.1%	3.3%
120	30	62.0	2.3%	1.8%	2.8%
120	40	132.0	2.3%	1.7%	2.9%
120	50	180.0	2.5%	1.8%	3.2%
120	60	215.0	2.9%	2.1%	3.7%
120	70	289.0	2.6%	1.8%	3.4%
120	80	365.0	2.4%	1.6%	3.2%
120	90	442.0	2.2%	1.5%	3.0%
120	100	515.0	2.1%	1.4%	2.9%
130	19	2.2	2.3%	1.7%	2.8%
130	20	3.2	2.5%	1.9%	3.0%
130	25	40.1	2.5%	2.0%	3.1%
130	30	89.2	2.3%	1.7%	2.8%
130	40	157.2	2.4%	1.7%	3.0%
130	50	205.2	2.7%	2.0%	3.5%
130	60	260.2	2.9%	2.0%	3.7%
130	70	355.2	2.4%	1.7%	3.2%
130	80	448.2	2.2%	1.4%	2.9%
130	90	532.2	2.1%	1.3%	2.8%
140	17	2.3	2.2%	1.7%	2.7%
140	20	16.3	2.6%	2.0%	3.2%
140	25	63.3	2.4%	1.9%	3.0%
140	30	113.3	2.3%	1.7%	2.8%
140	40	180.3	2.5%	1.8%	3.2%
140	50	221.3	3.1%	2.2%	3.9%
140	60	327.3	2.5%	1.7%	3.3%
140	70	428.3	2.2%	1.5%	3.0%
140	80	534.3	2.0%	1.3%	2.7%
150	14	2.5	1.8%	1.4%	2.3%
150	15	4.5	2.0%	1.5%	2.5%
150	20	28.5	2.7%	2.1%	3.3%
150	25	84.5	2.4%	1.8%	3.0%
150	30	133.5	2.3%	1.7%	3.0%
150	40	201.5	2.6%	1.9%	3.4%
150	50	269.5	2.8%	2.0%	3.7%
150	60	386.5	2.4%	1.6%	3.1%
150	70	512.5	2.0%	1.3%	2.7%
150	80	611.5	1.9%	1.2%	2.6%
160	12	2.7	1.6%	1.2%	2.0%
160	15	10.7	2.2%	1.7%	2.7%
160	20	44.7	2.7%	2.1%	3.3%
160	25	104.7	2.4%	1.8%	3.0%
160	30	151.7	2.5%	1.8%	3.1%
160	40	219.7	2.8%	2.0%	3.6%
160	50	330.6	2.5%	1.7%	3.3%
160	60	463.7	2.1%	1.4%	2.8%
170	11	2.8	1.6%	1.2%	2.0%
170	15	20.8	2.3%	1.8%	2.8%
170	20	60.8	2.7%	2.1%	3.3%
170	25	121.8	2.5%	1.8%	3.1%
170	30	168.8	2.6%	1.9%	3.3%
170	40	239.8	3.0%	2.1%	3.8%
170	50	387.8	2.3%	1.6%	3.0%
170	60	535.8	1.9%	1.3%	2.6%
180	10	3.0	1.5%	1.1%	1.9%
180	15	30.0	2.4%	1.8%	3.0%
180	20	77.0	2.7%	2.0%	3.3%
180	25	139.0	2.5%	1.9%	3.2%
180	30	185.0	2.7%	1.9%	3.4%
180	40	295.0	2.6%	1.8%	3.4%
180	50	449.0	2.1%	1.4%	2.8%
180	60	598.0	1.9%	1.2%	2.5%
190	9	3.2	1.4%	1.0%	1.8%
190	10	8.2	1.6%	1.2%	2.1%
190	15	38.2	2.5%	1.9%	3.1%
190	20	92.2	2.7%	2.0%	3.4%
190	25	156.1	2.6%	1.9%	3.3%
190	30	201.2	2.8%	2.0%	3.6%
190	40	346.2	2.4%	1.6%	3.1%

TABLE A3. DCS PROBABILITY FOR THE U.S. NAVY STANDARD AIR TABLE (USN57) ESTIMATED BY THREE PROBABILISTIC MODELS

Ascent rates are 30 fsw/min, except for estimates by the NMRI-93 Model

* = information not available

			By StandAir Model			By NMRI-98 Model			By NMRI-93 Model		
(1)	(2)	(3)	(4)	(5)	(6)	(7)	(8)	(9)	(10)	(11)	(12)
									60 fsw/min ascent rate		
Depth, fswg	Bottom time, min	TDT, min	*Pdcs*, %	Low CI, %	High CI, %	*Pdcs*, %	Low CI, %	High CI, %	*Pdcs*, %	Low CI, %	High CI, %
35	310	1.2	2.1	1.2	3	*	*	*	5.4	4.1	6.7
40	200	1.4	2.5	1.7	3.4	5.9	4.8	7.0	4.0	2.9	5.0
40	210	3.4	2.7	1.8	3.6	6.1	5.0	7.2	4.2	3.1	5.2
40	230	8.4	3	2	3.9	6.6	5.4	7.8	4.6	3.5	5.8
40	250	12.4	3.3	2.2	4.3	7.2	5.9	8.5	5.3	4.1	6.5
40	270	16.4	3.6	2.4	4.7	7.7	6.3	9.0	5.8	4.6	7.1
40	300	20.4	4.1	2.8	5.4	8.5	7.0	9.9	6.7	5.3	8.1
50	100	1.6	2.3	1.7	3	4.0	3.2	4.8	2.5	1.8	3.3
50	110	4.6	2.7	2	3.4	4.5	3.6	5.3	2.8	2.0	3.5
50	120	6.6	3.1	2.2	4	5.0	4.1	5.9	3.1	2.2	4.0
50	140	11.6	4	2.9	5.1	6.0	5.0	7.1	3.9	2.9	4.9
50	160	22.6	4.6	3.3	5.9	6.9	5.7	8.1	4.7	3.6	5.9
50	180	30.6	5.3	3.8	6.8	7.8	6.4	9.1	5.5	4.3	6.8
50	200	36.6	6.2	4.4	8	8.6	7.1	10.1	6.3	5.0	7.7
50	220	41.6	7.2	5.1	9.2	9.4	7.8	11.0	7.1	5.7	8.6
50	240	48.6	7.9	5.6	10.2	10.1	8.3	11.8	7.8	6.3	9.4
60	60	2.0	1.9	1.4	2.4	2.8	2.2	3.4	2.1	1.5	2.8
60	70	4.0	2.5	1.8	3.1	3.5	2.7	4.2	2.4	1.6	3.1
60	80	9.0	3	2.2	3.8	4.2	3.3	5.0	2.7	1.9	3.5
60	100	16.0	4.5	3.3	5.7	5.7	4.7	6.8	3.8	2.8	4.7
60	120	28.0	5.8	4.2	7.4	7.2	5.9	8.4	4.9	3.7	6.1
60	140	41.0	7	5	8.9	8.4	7.0	9.8	6.0	4.6	7.3
60	160	50.0	8.6	6.1	11.1	9.6	7.9	11.3	7.1	5.5	8.6
60	180	58.0	10.4	7.3	13.5	10.7	8.8	12.6	8.1	6.3	9.8
60	200	72.0	11.2	7.8	14.5	11.6	9.5	13.7	8.9	7.0	10.8
70	50	2.4	2.3	1.7	2.9	3.0	2.3	3.7	2.4	1.7	3.1
70	60	10.4	3	2.3	3.7	3.8	3.0	4.6	2.6	1.8	3.4
70	70	16.4	3.9	2.9	4.8	4.8	3.8	5.7	3.2	2.4	4.0
70	80	20.4	5	3.7	6.3	5.8	4.8	6.8	4.0	3.0	4.9
70	90	25.4	6.3	4.6	8	6.8	5.7	8.0	4.7	3.6	5.8
70	100	35.4	7.1	5.2	9	7.7	6.4	9.0	5.5	4.2	6.7
70	110	45.4	7.8	5.7	10	8.5	7.1	9.9	6.1	4.7	7.5
70	120	53.4	8.8	6.3	11.2	9.3	7.7	10.9	6.7	5.2	8.3
70	130	60.4	9.9	7.1	12.6	10.1	8.3	11.9	7.4	5.7	9.1
70	140	66.4	11.1	7.9	14.3	10.9	8.9	12.8	8.1	6.3	9.9

70	150	72.4	12.3	8.7	15.9	11.6	9.5	13.7	8.8	6.8	10.7
70	160	87.4	11.9	8.5	15.4	12.1	9.9	14.3	9.2	7.1	11.3
70	170	100.4	11.8	8.4	15.3	12.6	10.3	14.9	9.6	7.4	11.8
80	40	2.6	2.3	1.8	2.9	2.8	2.2	3.5	2.4	1.7	3.1
80	50	12.6	3.2	2.5	4	3.8	2.9	4.6	2.7	1.9	3.5
80	60	19.6	4.5	3.4	5.5	5.0	4.0	6.0	3.5	2.6	4.4
80	70	25.6	6	4.5	7.5	6.3	5.2	7.4	4.5	3.4	5.5
80	80	35.6	7.4	5.5	9.3	7.5	6.2	8.7	5.3	4.1	6.5
80	90	48.6	8.4	6.2	10.5	8.5	7.1	10.0	6.2	4.8	7.5
80	100	59.6	9.5	7	12	9.6	8.0	11.2	7.1	5.5	8.6
80	110	68.6	10.9	8	13.9	10.7	8.8	12.5	8.0	6.2	9.7
80	120	75.6	12.7	9.1	16.3	11.7	9.6	13.8	8.9	6.9	10.9
80	130	84.6	14.1	10.1	18.1	12.6	10.3	14.9	9.7	7.4	11.9
80	140	97.6	14.6	10.4	18.8	13.4	11.0	15.8	10.3	7.9	12.7
80	150	111.6	14.8	10.6	19.1	14.2	11.5	16.7	10.9	8.3	13.4
90	30	3.0	1.9	1.5	2.4	2.3	1.7	2.9	2.1	1.5	2.7
90	40	10.0	3.1	2.4	3.8	3.4	2.6	4.2	2.6	1.8	3.4
90	50	21.0	4.5	3.5	5.5	4.8	3.8	5.8	3.5	2.6	4.4
90	60	28.0	6.5	4.9	8	6.4	5.2	7.6	4.6	3.6	5.7
90	70	40.0	8.2	6.2	10.2	7.8	6.4	9.1	5.7	4.4	6.9
90	80	56.0	9.4	7.1	11.7	9.2	7.6	10.7	6.8	5.4	8.2
90	90	69.0	10.9	8.1	13.7	10.5	8.7	12.2	7.9	6.3	9.6
90	100	78.0	13.1	9.6	16.5	11.8	9.8	13.8	9.1	7.1	11.0
90	110	88.0	15.1	10.9	19.2	13.1	10.7	15.3	10.1	7.8	12.4
90	120	103.0	15.9	11.5	20.3	14.1	11.6	16.6	11.0	8.4	13.5
90	130	118.0	16.6	11.9	21.2	15.0	12.2	17.7	11.7	8.9	14.4
100	25	3.4	1.8	1.4	2.3	2.2	1.6	2.7	2.1	1.4	2.7
100	30	6.4	2.5	1.9	3.1	2.7	2.0	3.3	2.3	1.6	3.0
100	40	18.4	4	3.2	4.9	4.2	3.3	5.1	3.2	2.3	4.1
100	50	29.4	6.1	4.7	7.4	5.9	4.7	7.1	4.3	3.3	5.4
100	60	40.4	8.5	6.5	10.5	7.7	6.3	9.1	5.7	4.4	6.9
100	70	59.4	9.9	7.5	12.3	9.3	7.8	10.9	7.1	5.6	8.5
100	80	74.4	11.8	8.9	14.7	11.0	9.1	12.8	8.5	6.7	10.2
100	90	86.4	14.2	10.5	17.8	12.5	10.3	14.6	9.7	7.7	11.8
100	100	99.4	16.3	12	20.6	14.0	11.5	16.4	11.0	8.5	13.3
100	110	119.4	16.7	12.2	21.2	15.2	12.5	17.8	11.9	9.1	14.6
100	120	134.4	18	13.1	23	16.4	13.4	19.4	12.9	9.9	15.8
110	20	3.6	1.6	1.2	2	1.9	1.4	2.4	1.9	1.2	2.5
110	25	6.6	2.3	1.8	2.8	2.4	1.8	3.0	2.2	1.5	2.9
110	30	10.6	3.2	2.5	3.9	3.2	2.5	4.0	2.7	1.9	3.5
110	40	26.6	5.1	4.1	6.2	5.0	3.9	6.1	3.8	2.7	4.8
110	50	37.6	7.9	6.2	9.7	7.1	5.8	8.5	5.3	4.0	6.5
110	60	57.6	9.9	7.7	12.2	9.1	7.5	10.6	6.9	5.5	8.4
110	70	75.6	12.1	9.2	15	11.0	9.2	12.8	8.6	6.9	10.3
110	80	90.6	14.7	11	18.4	12.8	10.6	15.0	10.1	8.1	12.1
110	90	109.6	16.3	12.1	20.5	14.5	12.0	16.9	11.5	9.1	13.9
110	100	127.6	17.9	13.1	22.7	16.1	13.2	18.8	12.8	9.9	15.6
120	15	4.0	1.2	0.9	1.6	1.5	1.1	2.0	1.6	1.0	2.2
120	20	6.0	1.9	1.5	2.4	2.1	1.5	2.6	2.0	1.4	2.7
120	25	10.0	2.9	2.2	3.5	2.9	2.2	3.6	2.5	1.7	3.2
120	30	18.0	3.9	3.1	4.7	3.9	2.9	4.8	3.1	2.1	4.0

120	40	34.0	6.4	5.1	7.8	6.0	4.7	7.2	4.4	3.3	5.6
120	50	50.0	9.5	7.4	11.6	8.4	6.8	9.9	6.4	5.0	7.8
120	60	73.0	11.6	9	14.3	10.5	8.7	12.3	8.3	6.6	9.9
120	70	91.0	14.5	11	18	12.7	10.5	14.8	10.1	8.2	12.1
120	80	109.0	17.2	12.8	21.6	14.8	12.2	17.2	11.9	9.5	14.3
120	90	134.0	18.1	13.3	22.8	16.5	13.7	19.3	13.3	10.4	16.2
120	100	152.0	20.2	14.7	25.7	18.3	15.0	21.6	14.8	11.5	18.0
130	10	4.4	0.8	0.6	1.1	1.2	0.7	1.6	1.3	0.7	1.9
130	15	5.4	1.4	1	1.8	1.7	1.1	2.2	1.7	1.1	2.4
130	20	8.4	2.3	1.8	2.8	2.4	1.7	3.0	2.2	1.5	2.9
130	25	14.4	3.5	2.7	4.2	3.4	2.5	4.2	2.8	2.0	3.7
130	30	25.4	4.6	3.7	5.5	4.4	3.4	5.4	3.4	2.4	4.4
130	40	39.4	8.1	6.4	9.9	7.1	5.6	8.4	5.3	4.0	6.6
130	50	65.4	10.6	8.3	13	9.5	7.8	11.2	7.4	5.8	8.9
130	60	88.4	13.4	10.2	16.5	12.0	10.0	14.0	9.6	7.8	11.4
130	70	105.4	17.2	12.9	21.5	14.2	11.7	16.6	11.8	9.5	14.1
130	80	133.4	18.3	13.5	23	16.6	13.7	19.3	13.5	10.7	16.2
130	90	156.4	20.1	14.7	25.5	15.8	13.2	18.4	15.1	11.9	19.3
140	10	4.6	0.9	0.6	1.2	1.3	0.8	1.8	1.4	0.8	2.0
140	15	6.6	1.7	1.2	2.1	1.8	1.3	2.4	1.9	1.2	2.5
140	20	10.6	2.8	2.2	3.4	2.7	2.0	3.4	2.4	1.7	3.2
140	25	20.6	4	3.2	4.9	3.8	2.9	4.8	3.1	2.1	4.0
140	30	30.6	5.6	4.4	6.7	5.1	4.0	6.3	3.9	2.0	4.3
140	40	48.6	9.6	7.5	11.7	8.0	6.5	9.6	6.2	4.7	7.6
140	50	78.6	12.1	9.4	14.8	10.8	8.9	12.7	8.6	6.8	10.3
140	60	99.6	16	12.1	19.8	13.7	11.3	16.0	11.2	9.0	13.2
140	70	127.6	18.1	13.4	22.7	16.1	13.4	18.8	13.2	10.7	15.8
140	80	157.6	19.3	14.1	24.4	18.4	15.2	21.5	15.1	12.0	18.1
150	20	14.0	3.3	2.6	4	3.1	2.2	3.9	2.6	1.0	2.6
150	25	26.0	4.7	3.8	5.7	4.4	3.3	5.4	3.4	2.3	4.4
150	30	37.0	6.5	5.2	7.9	5.9	4.6	7.2	4.4	3.2	5.7
150	40	62.0	10.4	8.1	12.7	9.0	7.3	10.7	7.0	5.4	8.6
150	50	91.0	13.7	10.5	16.9	12.2	10.0	14.2	9.9	7.9	11.8
150	60	115.0	17.7	13.3	22.1	15.2	12.6	17.7	12.6	10.2	14.9
150	70	149.0	19	14	24.1	17.9	14.8	20.8	14.8	11.8	17.6
150	80	176.0	21.4	15.5	27.4	20.4	16.8	23.9	17.0	13.5	20.3
160	5	5.4	0.6	0.3	0.8	0.9	0.5	1.4	1.1	0.5	1.7
160	10	6.4	1.2	0.8	1.5	1.5	1.0	2.0	1.6	0.9	2.2
160	15	10.4	2.2	1.7	2.8	2.3	1.6	3.0	2.1	1.4	2.8
160	20	19.4	3.7	2.9	4.5	3.5	2.5	4.6	2.9	1.9	3.7
160	25	32.4	5.4	4.3	6.5	5.1	3.7	6.5	3.8	2.6	4.9
160	30	43.4	7.6	6	9.2	6.8	5.1	8.4	5.0	3.6	6.4
160	40	74.4	11.4	8.8	13.9	9.7	7.6	11.7	8.0	6.2	9.8
160	50	101.4	15.7	11.9	19.6	13.8	11.3	16.2	11.2	9.0	13.2
160	60	135.4	18.2	13.5	23	17.0	14.2	19.7	13.9	11.3	16.4
170	5	5.6	0.6	0.4	0.8	1.0	0.5	1.5	1.1	0.5	1.8
170	10	7.6	1.3	0.9	1.7	1.6	1.0	2.2	1.6	1.0	2.3
170	15	12.6	2.5	1.9	3.1	2.6	1.8	3.4	2.2	1.5	2.9
170	20	24.6	4.2	3.3	5.1	4.1	2.9	5.2	3.1	2.1	4.1
170	25	37.6	6.2	4.9	7.5	5.8	4.3	7.3	4.1	2.9	5.4
170	30	48.6	8.9	6.9	10.8	7.8	6.0	9.6	5.6	4.1	7.2

170	40	84.6	12.7	9.7	15.6	11.7	9.4	13.9	9.0	7.0	10.9
170	50	112.6	17.6	13.1	22.1	15.6	12.9	18.2	12.5	10.1	14.8
170	60	155.6	18.7	13.7	23.8	18.8	15.9	21.7	15.2	12.4	17.9
180	5	6.0	0.6	0.4	0.9	1.1	0.6	1.6	1.2	0.5	1.8
180	10	9.0	1.4	1	1.8	1.8	1.2	2.3	1.7	1.0	2.4
180	15	15.0	2.9	2.2	3.6	2.9	2.1	3.8	2.4	1.6	3.2
180	20	29.0	4.7	3.7	5.8	4.6	3.4	5.9	3.3	2.2	4.4
180	25	43.0	7.1	5.5	8.6	6.6	5.0	8.3	4.6	3.2	6.0
180	30	56.0	10	7.7	12.2	8.8	6.9	10.8	6.4	4.6	8.1
180	40	96.0	13.7	10.4	17.1	13.1	10.6	15.4	10.0	7.9	12.1
180	50	131.0	17.9	13.1	22.6	17.2	14.3	19.9	13.6	11.1	16.0
180	60	171.0	20.2	14.5	25.9	21.0	17.8	24.0	16.7	13.6	19.6
190	5	6.4	0.7	0.4	0.9	1.2	0.7	1.7	1.2	0.6	1.9
190	10	10.4	1.6	1.2	2	1.9	1.3	2.5	1.7	1.0	2.4
190	15	17.4	3.3	2.5	4	3.3	2.4	4.3	2.5	1.7	3.4
190	20	34.4	5.3	4.1	6.4	5.2	3.8	6.6	3.6	2.4	4.7
190	25	47.4	8.1	6.2	10	7.5	5.8	9.3	5.2	3.6	6.7
190	30	66.4	10.6	8.1	13.1	9.9	7.7	11.9	7.0	5.2	8.9
190	40	106.4	15	11.2	18.9	14.5	11.9	17.1	11.1	8.8	13.3